BRANZ

STUDY REPORT

No. SR 180 (2007)

Air Flow Rates
Field Measurements

L Quaglia

M Cunningham

The work reported here was funded by Building Research Levy and partially funded by the Department of Building and Housing.

ISSN: 0113–3675

Preface

This report provides a description of experimental results obtained during a study of air flow patterns in residential dwellings using a multi-tracer gas technique. The information reported relates the findings of the first stage of a research program aimed to study the properties and the functioning of building underlays under New Zealand conditions.

Acknowledgments

This work was funded by the Building Research Levy and partially funded by the Department of Building and Housing.

Note

This report is intended primarily for others researchers interested in ventilation rates in roof cavities.

AIR FLOW RATES FIELD MEASUREMENTS

BRANZ Study Report SR 180 (2007) L Quaglia and M Cunningham

Reference

Quaglia L and Cunningham M. 2007. 'Air Flow Rates Field Measurements'. BRANZ *Study Report 180(2007)*. BRANZ Ltd, Judgeford, New Zealand.

Abstract

Ventilation plays a key role in the process of moisture formation and removal in roof envelopes. In order to investigate patterns and magnitude of air flows affecting the behaviour of roofs (with a special focus on building underlays), a field device has been designed and developed. This apparatus provides all the data needed to estimate air flow rates and it is based on an implementation of the constant concentration multi-tracer gas method.

The apparatus was used for a campaign of field measurements in private residential dwellings. Several typologies of measurements are presented: measurements of air flow rates between roof space and living space; measurements of air flows between roof space and cavity underlay-cladding; and measurements of air flow direction inside the cavity underlay-cladding.

Keywords

Air flow rates, building underlay, roof space, tracer gas measurements, ventilation.

Contents Page

Figures

1. INTRODUCTION

Mass transfer due to air flows is one of the most important transport processes of heat and moisture in a building. Air movements take place between indoors and outdoors and between different zones within the building, and they are driven by pressure gradients generated by wind and temperature differences.

In the experimental programme to determine the required properties of building underlays, measurements of air flow rates are important in order to understand the role of ventilation (adventitious or forced) on their functioning. In this context, ventilation plays a key role in the process of moisture formation and removal in the roof envelope.

Most of the measurements of ventilation rates are accomplished using tracer gases (Trechsel 1994). One or more tracer gases are released in the building and their concentration is measured in different locations of the edifice at regular time intervals. Air movements drive the tracer gases towards outdoors and towards zones different from the ones where the tracer gases have been released. The magnitude of air flows can then be theoretically estimated from the knowledge of the concentrations. This is achieved making use of the equation of conservation of mass of tracer gas applied to each of the zones in which the building has been subdivided.

In order to carry out these measurements, a field device was designed and developed for use in private dwellings and in a test building. This apparatus accomplishes two tasks. The first task is to allow the injection of tracer gases and the sampling of air from three different zones. The second task is to measure the concentration of the three different tracer gases in the air samples drawn from each zone.

This report is divided into three sections: the first deals with the multi-tracer gas method of measuring air flows; the second gives details about the apparatus and other instruments used; the third presents some of the experimental results obtained during the campaign of field measurements of ventilation rates.

2. TRACER GAS METHOD

2.1 Typologies of implementation

There exist several ways of implementing tracer gas measurements (Trechsel 1994). According to the number of tracer gases used, we have the single-tracer method and the multi-tracer method. If the building is considered as a whole, and then only the air flows between indoors and outdoors are of interest, using a single-tracer gas is enough to estimate the air flow magnitudes. On the contrary, if the building is thought of as subdivided into zones (i.e. the main living space and the roof space), and the magnitude of the air flows within zones needs to be calculated, it is essential to use several tracer gases, one for each zone (see Figure 1).

According to the way the tracer gas is injected we have: the decay method; the constant injection method; and the constant concentration method (see Figure 2). With the decay method, a certain quantity of tracer gas is quickly injected into a zone of the building and the decay of the concentration is observed. The rate of decay is directly related to the air flow from the zone towards outdoors or other zones. With the constant injection method, the injection rate is kept constant during the whole measurement. Variations of the concentration of tracer gases are directly related to variations of the flow rates. With the constant concentration method, the injection rate is adjusted at regular time intervals in order to maintain the concentration of tracer gases as constant as possible during the whole measurement. Variations of the injection rates are directly related to variations of the flow rates. This method requires a control system for the

injection and a suitable algorithm to calculate the approximate quantity of tracer gases to inject in order to keep the concentrations constant.

The multi-tracer constant injection method was chosen to perform the measurements in the field. This choice was motivated by the fact that it is much easier to implement this method than the constant concentration method. The drawback of the constant injection method is that it can lead to erroneous estimations of the ventilation rates if the magnitude of air flows is changing very rapidly.

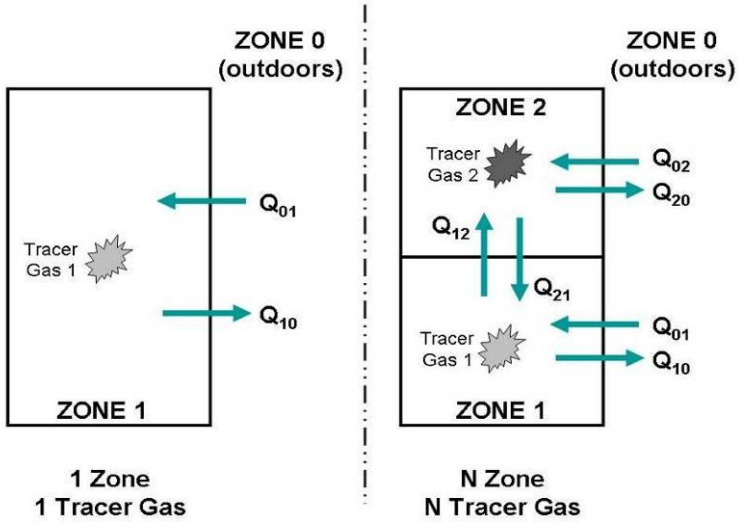

Figure 1. Single-tracer method (on the left) vs. multi-tracer method (on the right).

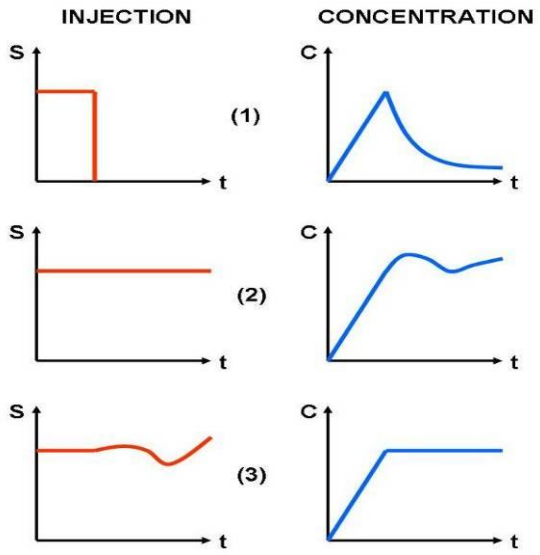

Figure 2. Typologies of tracer gas methods. (1) Decay method (2) Constant injection method (3) Constant concentration method. For each couple of graphs, the left one represents the dependency of the injection rate with time (S = "source"), the right one represents the dependency of the concentration of tracer gas with time (C = "concentration").

2.2 Mass continuity equations

Conservation equations for the mass of air and of tracer gases allow calculating air flow rates from concentration measurements (Roulet 1989). Let's consider a volume V

containing a certain tracer gas and observe it during a time interval Δt (see Figure 3). Tracer gas is brought into the volume by air flows from the outside (infiltration) and it is removed from the volume by air flows towards the outside (exfiltration). Sometimes a source of tracer gas can be present in the volume (injection). Due to these three processes, the mass of tracer gas in the volume usually varies during the time interval Δt.

The general mass conservation equation states that the variation in mass in the time interval Δt of tracer gas in the volume V is equal to the mass of tracer gas injected into the volume V during the time interval Δt plus the mass of tracer gas carried by the air entering the volume V during the time interval Δt minus the mass of tracer gas carried by the air exiting the volume V during the time interval Δt.

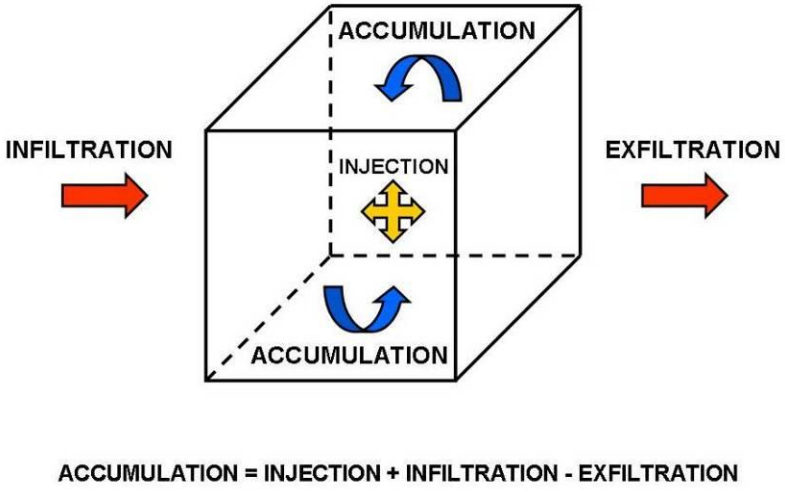

.

Figure 3. Terms contributing to the general mass conservation equation: mass entering the volume ("infiltration"), mass exiting the volume ("exfiltration"), accumulation of mass in the volume ("accumulation") and source term ("injection").

In the case of a building, the volume V can be the whole edifice or one of the zones in which the building has been subdivided for the measurement. The infiltration can be thus split into the air flows coming from outdoors and from each of the other zones. Similarly, the exfiltration can be split into the air flows going towards outdoors and towards each of the other zones.

If there is only one zone (indexed 1), one tracer gas is enough to determine the total air flow rates in and out the zone (the outside is indexed 0). If we call $Q_{1\to0}$ (m^3/s) the air flow rate from the zone towards outdoors, $Q_{0\to1}$ (m^3/s) the air flow rate from outdoors towards the zone, c_1 (kg/m^3) and c_0 (kg/m^3) the concentration of tracer gas in the zone and outdoors (background), and S (kg/s) the intensity of the injection of tracer gas, the continuity equation for the mass of tracer gas takes the form:

$$V\dot{c}_1 = S + (c_0 - c_1)Q_{0\to1} \tag{2.1}$$

$$Q_{1\to0} = Q_{0\to1} \tag{2.2}$$

where $\dot{c}$ indicates the time derivative of the concentration.

If the building is subdivided in N zones, N different tracer gases are needed in order to determine the magnitude of the air flow rates among zones. In each zone only one tracer gas is injected and a different tracer gas is injected in each zone. In this case, it is possible to write N conservation equations, one for each tracer gas. They take the following form:

$$V_i \dot{c}_i^{(k)} = S_i^{(k)} + \sum_{j=0}^{N} (c_j^{(k)} - c_i^{(k)}) Q_{j \to i} \bar{\delta}_{ij} \tag{2.3}$$

$$Q_{i \to 0} = \sum_{j=0}^{N} Q_{j \to i} \bar{\delta}_{ij} - \sum_{j=1}^{N} Q_{i \to j} \bar{\delta}_{ij} \tag{2.4}$$

where the superscript k identifies the tracer gas ($k = 1..N$), i, j indicate the zones ($i, j = 0..N$) and

$$\bar{\delta}_{ij} \begin{cases} = 0 \text{ if } i = j \\ = 1 \text{ if } i \neq j \end{cases} \tag{2.5}$$

Usually the intensities of the injection of the different tracer gases are kept constant during the time (Sandberg 1989). Moreover, if the concentrations are not changing too quickly, the time derivates in the conservations equations can be set equal to zero. With these assumptions and taking N=2 as an example, we obtain:

$$S_1^{(1)} + (c_0^{(1)} - c_1^{(1)}) Q_{0 \to 1} + (c_2^{(1)} - c_1^{(1)}) Q_{2 \to 1} = 0 \tag{2.6}$$

$$(c_0^{(2)} - c_1^{(2)}) Q_{0 \to 1} + (c_2^{(2)} - c_1^{(2)}) Q_{2 \to 1} = 0 \tag{2.7}$$

$$(c_0^{(1)} - c_2^{(1)}) Q_{0 \to 2} + (c_1^{(1)} - c_2^{(1)}) Q_{1 \to 2} = 0 \tag{2.8}$$

$$S_2^{(2)} + (c_0^{(2)} - c_2^{(2)}) Q_{0 \to 2} + (c_1^{(2)} - c_2^{(2)}) Q_{1 \to 2} = 0 \tag{2.9}$$

$$Q_{1 \to 0} = Q_{0 \to 1} + Q_{2 \to 1} - Q_{1 \to 2} \tag{2.10}$$

$$Q_{2 \to 0} = Q_{0 \to 2} + Q_{1 \to 2} - Q_{2 \to 1} \tag{2.11}$$

For easiness of computation, the first four of these equations can be rearranged as two separate linear systems:

$$\begin{bmatrix} (c_1^{(1)} - c_0^{(1)}) & (c_1^{(1)} - c_2^{(1)}) \\ (c_1^{(2)} - c_0^{(2)}) & (c_1^{(2)} - c_2^{(2)}) \end{bmatrix} \begin{pmatrix} Q_{0 \to 1} \\ Q_{2 \to 1} \end{pmatrix} = \begin{pmatrix} S_1^{(1)} \\ 0 \end{pmatrix} \tag{2.12}$$

$$\begin{bmatrix} (c_2^{(1)} - c_0^{(1)}) & (c_2^{(1)} - c_1^{(1)}) \\ (c_2^{(2)} - c_0^{(2)}) & (c_2^{(2)} - c_1^{(2)}) \end{bmatrix} \begin{pmatrix} Q_{0 \to 2} \\ Q_{1 \to 2} \end{pmatrix} = \begin{pmatrix} 0 \\ S_2^{(2)} \end{pmatrix} \tag{2.13}$$

Knowing the concentration of the two tracer gases in each zone and the level of background concentration, it is now straightforward to compute the six air flow rates. If N=3, three separate linear systems are to be solved.

2.3 Choice of zones

The nature of air flows around a roof underlay and the geometry of roof envelopes have motivated the choice of using a multi-tracer gases technique. It is important to identify the zones of the building where air flows affect the behaviour of the roof underlay.

In the case of pitched roofs (see Figure 4), we can identify three zones: the cavity between the roof underlay and the cladding (Zone 1); the roof space (Zone 2); and the rest of the building (Zone 3). In the case of skillion roofs (see Figure 5), we can identify the following zones: the cavity between the roof underlay and the cladding (Zone 1); the cavity between roof underlay and insulation (Zone 2a); the insulation (Zone 2b); and the rest of the building (Zone 3). For skillion roofs, either Zone 2a or Zone 2b can be chosen as the zone lying underneath the underlay.

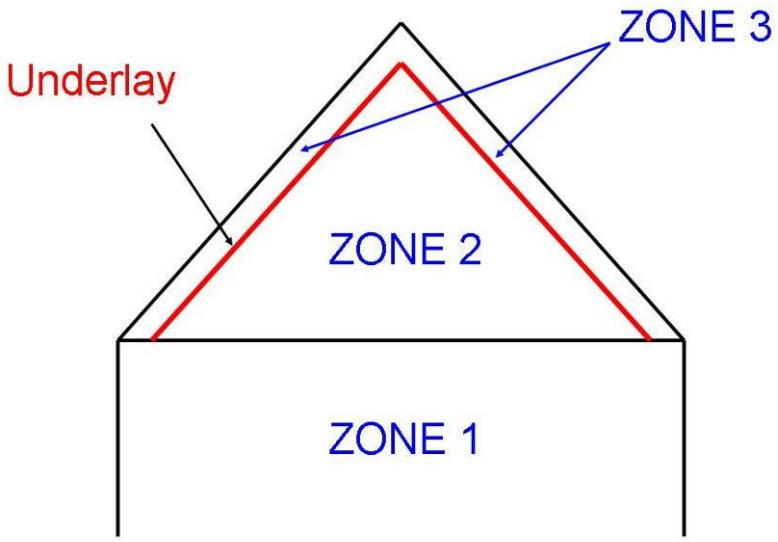

.

Figure 4. Example of possible subdivision in zones in the case of a dwelling with roof space.

In both geometries we have three major zones. We then need three different tracer gases (one to inject in each zone) in order to be able to measure the magnitude of all the possible air flows between the zones. The three tracer gases selected are: carbon dioxide (CO_2); nitrous oxide (N_2O); and isobutylene (C_4H_8). CO_2 and N_2O are commonly used as tracer gases in buildings and they are relatively easy to detect. C_4H_8 is a bit more unusual but it was selected because it can be easily detected with high accuracy.

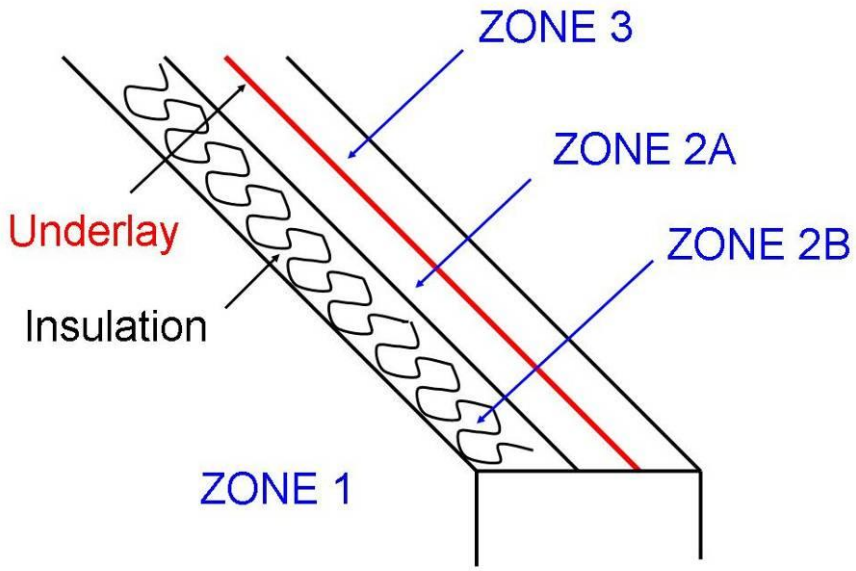

Figure 5. Example of possible subdivision in zones in the case of a dwelling with skillion roof.

3. INSTRUMENTATION

3.1 Air leakage apparatus

In order to accomplish the task of measuring air flows in the roof envelope using the multi-tracer constant injection method, we have designed and developed an apparatus that we will call the “air leakage apparatus”.

The two main tasks required by this apparatus are: 1) to be able to draw air samples from different zones of a building and then to return them back to the corresponding zone; and 2) to measure the concentration of CO_2, N_2O and C_4H_8 in the air sample.

In order to transport to the detectors the air samples to analyse and to deliver the tracer gases into the different zones, we use a set of small diameter polyurethane tubes. In each line, the air samples and the tracer gases are circulated using a low flow rate diaphragm pump (see Figure 6). This ensures that the air sample is always up-to-date. An advantage of using independent diaphragm pumps is that the flow rate can be adjusted to fit to the needs of the injection rate of the different tracer gases (these differences arise from the fact that the zones have different volumes and the magnitude of the natural air flows is different).

The injection of tracer gas is performed on the returning line using a system formed by a pressure regulator, a flow meter and a capillary tube in order to obtain a very low flow rate at the outlet of the gas bottle. This flow rate has to be lower than the flow rate generated by the diaphragm pumps in order to have good mixing with the air sample.

The air leakage apparatus cyclically measures the concentration of tracer gases in each of the three lines, one at a time and usually averaging over a period of one minute. In order to select a specific sampling line the apparatus relies on a system of 3-port solenoid valves, manifolds and bypasses as schematically illustrated in Figure 7.

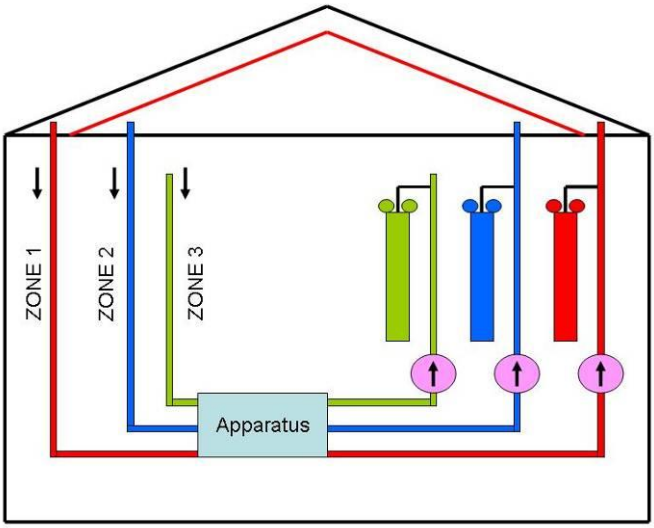

Figure 6. Set-up for the tracer gas method. Diaphragm pumps (inside the apparatus) circulate air samples from the zones to the detectors (inside the apparatus) back to the zones. The injection takes place on the returning lines.

Two banks of solenoid valves are mounted on two separate manifolds. Each solenoid valve can direct the air flow towards a manifold (when in the energised state) or towards a bypass (when in the de-energised state). Pairs of solenoid valves (each on a different manifold and connected to the same line) are wired together to the same digital channel of a Labjack so that they can be opened and shut simultaneously. The Labjack is a simple analogue and digital input/output unit that enables the communication between a computer and electronic devices.

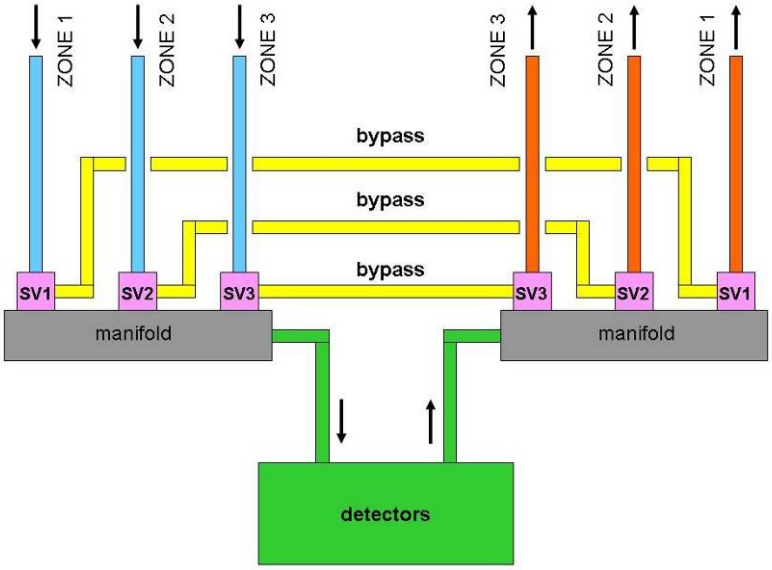

Figure 7. Set-up of solenoid valves allowing switching between zones. Detection takes place for air samples coming from a particular zone while air samples are kept circulating in all the lines through bypasses.

At any time, only one couple of solenoid valves is energised (the “active line”) while all the others are in the de-energised state (“bypassing lines”). In this case only the air sample in the active line goes into the manifold, through the detectors and back to the zone of origin. By cyclically opening and shutting pairs of solenoid valves it is then possible to measure the concentrations of tracer gases in the different zones at regular times

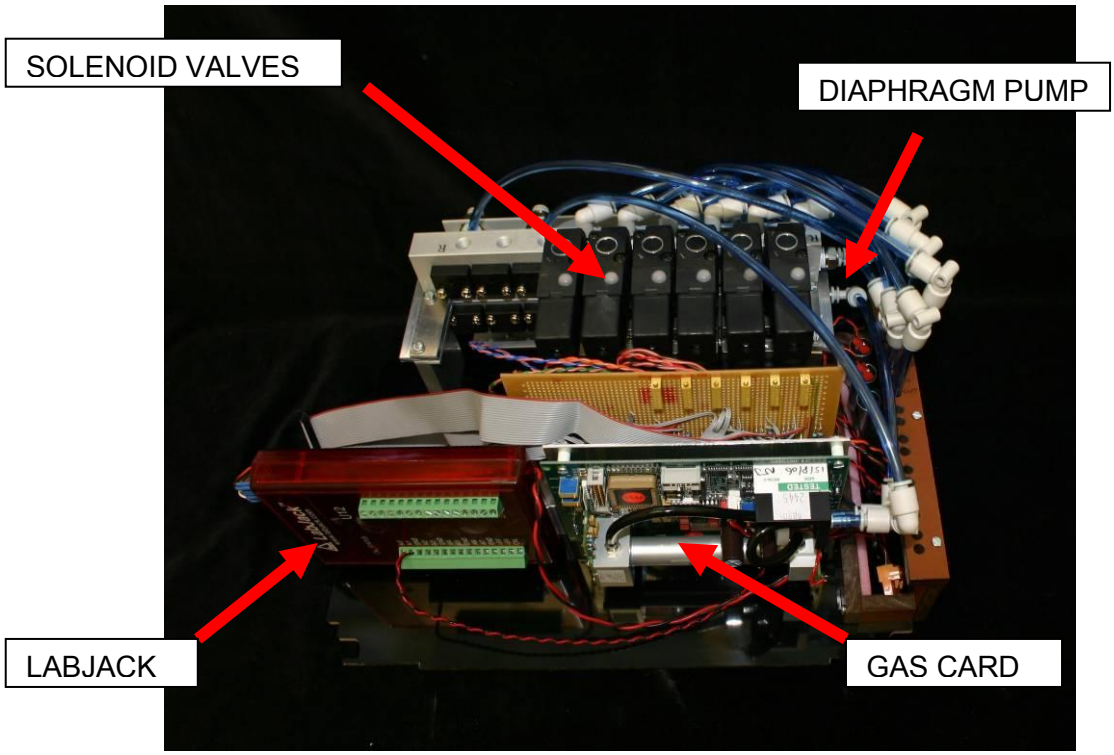

Figure 8. Picture of the air leakage apparatus which usually resides in a plastic box.

The three tracer gases are detected with three separate detectors. These detectors are selective to a specific tracer gas and they do not interfere with each other. The concentration of CO_2 and of N_2O is measured using a non-dispersive infrared detector (NDIR), the concentration of C_4H_8 using a photo-ionisation detector (PID).

The general schematic of an NDIR is depicted in Figure 9. CO_2 and N_2O have a strong absorption band in the infrared, at about 4.26µm and 4.55µm respectively. Due to these strong absorption bands, when the light coming from a polychromatic infrared source passes through an air sample containing CO_2 or N_2O, part of the light is absorbed. This light is then filtered in order to isolate the component at the wavelength of the specific absorption band. The intensity of this light is then compared with the intensity of the infrared source and the concentration of the specific gas can be calculated. The process of filtering the absorbed light at the wavelength of the absorption band allows achieving selectivity to a specific molecule.

The general schematic of a PID is depicted in Figure 10. C_4H_8 and many other volatile organic compounds have an ionisation potential less than 10.6 eV. Most of the molecules which are found in the normal composition of air (nitrogen, oxygen, argon, CO_2, N_2O …) have an ionisation potential greater than 10.6 eV. When illuminating the air sample with ultraviolet light at 117 nm (= 10.6 eV), only the molecules with an ionisation potential less than 10.6 eV are ionised. The electric charges produced by the ionisation are then collected using a couple of electrodes and the intensity of the electric current is measured. This intensity is directly proportional to the concentration of volatile organic compounds (in our case C_4H_8).

The non-dispersive infrared detector for N_2O is a GasCard II Plus by Edinburgh Instruments (see Figure 8). The GasCard, the Labjack, the solenoid valves banks, and the diaphragm pumps are all assembled in a box. The non-dispersive infrared detector for CO_2 and the photo-ionisation detector for C_4H_8 are bound into an IAQRae unit by Rae Systems (see Figure 11), which is then joined to the main box of the apparatus in order to close the air circuit.

Software written in Labview has been developed to control the air leakage apparatus. A screenshot of the main routine of the program is shown on Figure 12. The main tasks of the program are to command the opening and shutting of the solenoid valves and to synchronise this with the measurements of tracer gas concentrations.

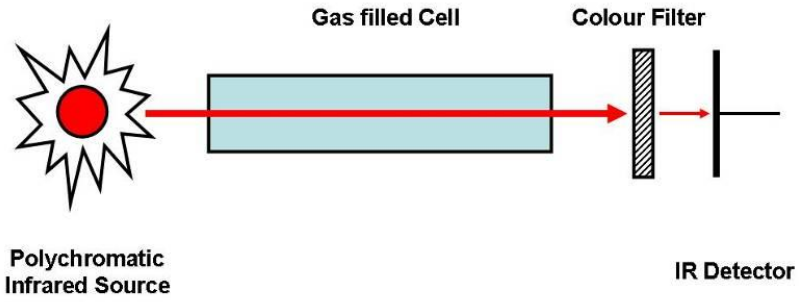

Figure 9. Schematic of a non-dispersive infrared detector.

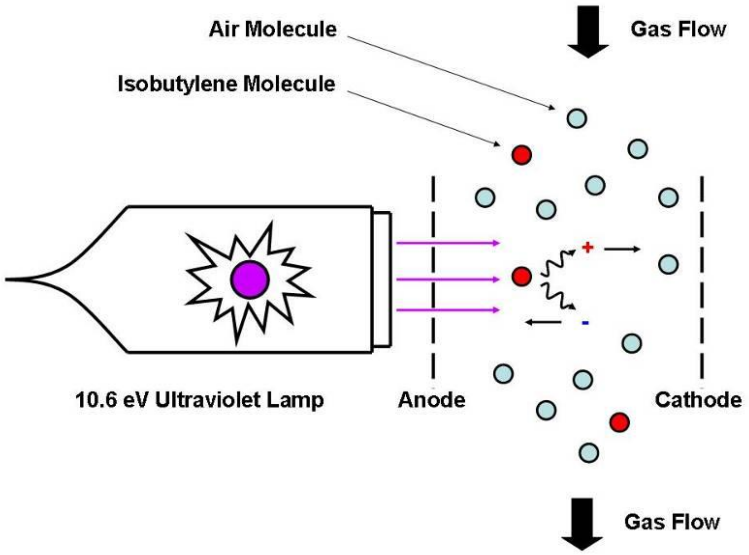

Figure 10. Schematic of a photo ionisation detector.

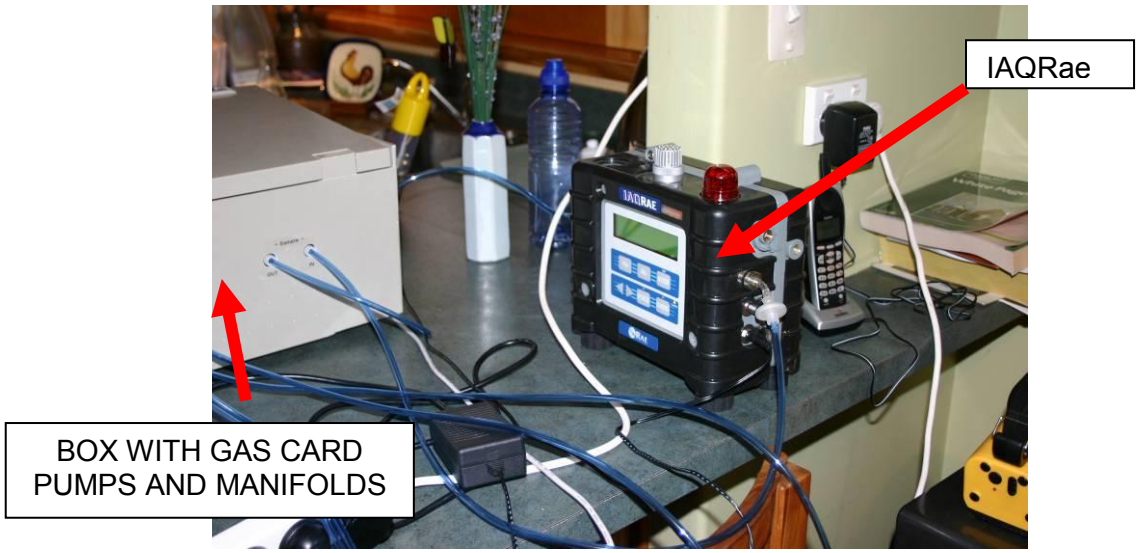

Figure 11. Picture of the IAQRae unit containing the photo ionisation detector for C_4H_8 and the non-dispersive infrared detector for CO_2.

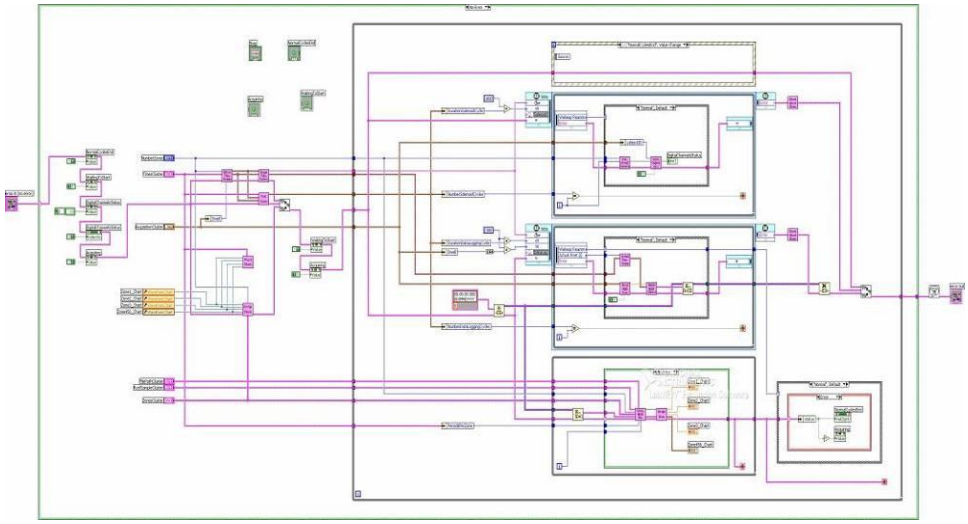

Figure 12. Screenshot of the main routine of the Labview program controlling the acquisition system and commanding the solenoid valves.

3.2 Meteorological and temperature monitoring

Air flows are driven by pressure gradients which are in turn generated by wind and temperature differences. So, in order to have a better picture of the tracer gas measurements we have monitored wind speed, wind direction and several temperatures (i.e. outdoors, in the roof space).

We used a weather station to gather meteorological data. The weather station used is a wireless Vantage Pro 2 equipped with a WeatherLink data logger by Davis Instruments. The weather station is composed of an integrated sensor suite (see Figure 13), and of a console (see Figure 15). The integrated sensor suite contains a temperature and a relative humidity sensor installed inside a solar radiation shield, an abrometer, a tipping bucket rain gauge and an anemometer. The anemometer is provided with a 12 m cable and can be mounted on a site different from the one of the integrated sensor suite. The anemometer is usually installed on the roof. The sensors

and the transmitter are powered by solar panels. The console receives data, displays them on screen and logs them into the data logger.

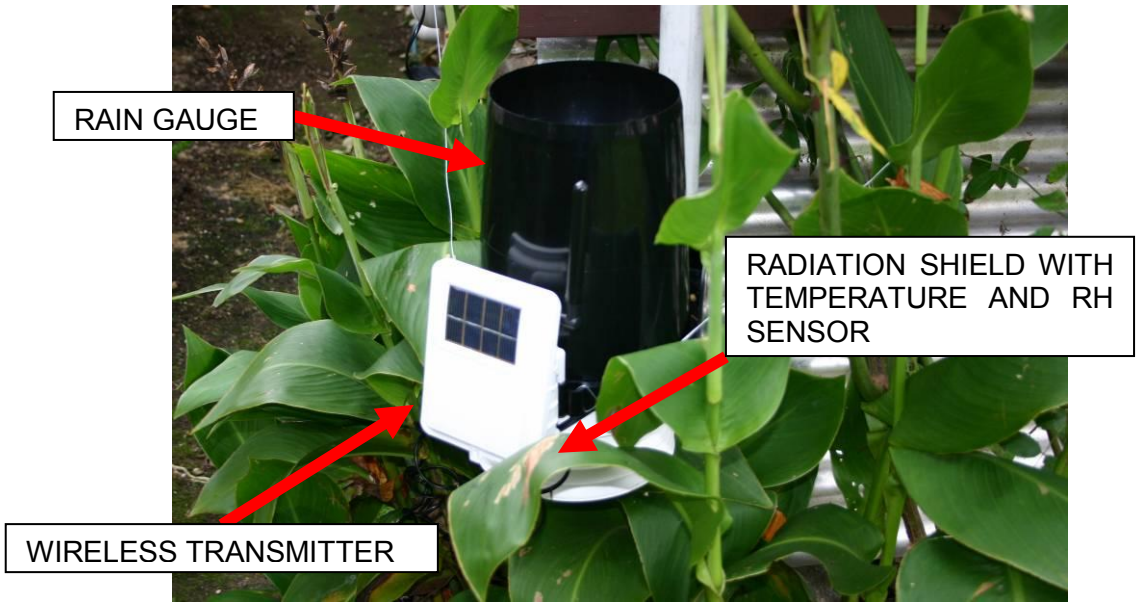

Figure 13. Integrated sensor suite of the weather station Vantage Pro 2 by Davis Instruments.

Figure 14. Anemometer mounted on the roof of one of the houses monitored.

Meteorological data were collected at five minute intervals. Wind data were then analysed using hourly vector averages (which is the same time average used to analyse tracer gas concentrations). From a sequence of 12 observations of wind speed U_i and wind direction θ_i (measured in degrees, clockwise starting from north), the mean east-west and north-south components of the wind vector are calculated:

$$V_{e-w} = \frac{1}{12}\sum_{i=1}^{12} U_i \sin(\vartheta_i) \qquad (3.1)$$

Figure 15. Console receiving data from the integrated sensor suite of the weather station. The data logger is located at the back of the console.

Figure 16. BRANZ temperature logger.

$$V_{n-s} = \frac{1}{12}\sum_{1}^{12} U_i \cos(\vartheta_i) \tag{3.2}$$

The mean wind speed and direction are then computed in the following way:

$$\overline{U} = \sqrt{V_{e-w}^2 + V_{n-s}^2} \tag{3.3}$$

$$\overline{\vartheta} = \arctan\left(\frac{V_{e-w}}{V_{n-s}}\right) + \Phi \tag{3.4}$$

where arctangent is defined from 0 to 360° (using the signs of V_{e-w} and V_{n-s}) and Φ is:

$$\Phi \begin{cases} = +180 \text{ if } \arctan(V_{e-w}/V_{n-s}) < 180 \\ = -180 \text{ if } \arctan(V_{e-w}/V_{n-s}) > 180 \end{cases} \quad (3.5)$$

Outside temperature was measured using the weather station. Temperatures inside the dwellings were measured using temperature loggers developed at BRANZ (Figure 16). These loggers contain a temperature sensor and a microprocessor. The microprocessor was programmed to acquire temperatures every five minutes and to store the reading in memory. The series of readings were then downloaded and processed at a later date.

4. EXPERIMENTAL RESULTS

4.1 Introduction

During the months of February, March and April 2007, measurements using the air leakage apparatus were carried out in several private dwellings. Inside each house we installed the apparatus, a computer for data logging (see Figure 17), and a network of small bore polyurethane tubes (see Figure 18) to continuously inject tracer gases and draw air samples and the BRANZ temperature loggers. Outside the house, we installed the gas cylinders to supply tracer gases (see Figures 19 and 20) and the weather station.

Due to the invasiveness of the experimental set-up, and in order to limit the effect of the opening and closing of doors and windows, all measurements have been performed while the occupants of the dwellings were not present, usually for a period of one to three weeks.

In the following paragraphs, we report some of the experimental results obtained in the different dwellings. For each measurement, we display graphs of several observables during the same timeframe. These observables are usually: hourly vectorial averages of wind speed and direction; temperature inside the house, in the roof space, and outdoors; concentration of each tracer gas in each zone; and, when meaningful, calculated air flow rates.

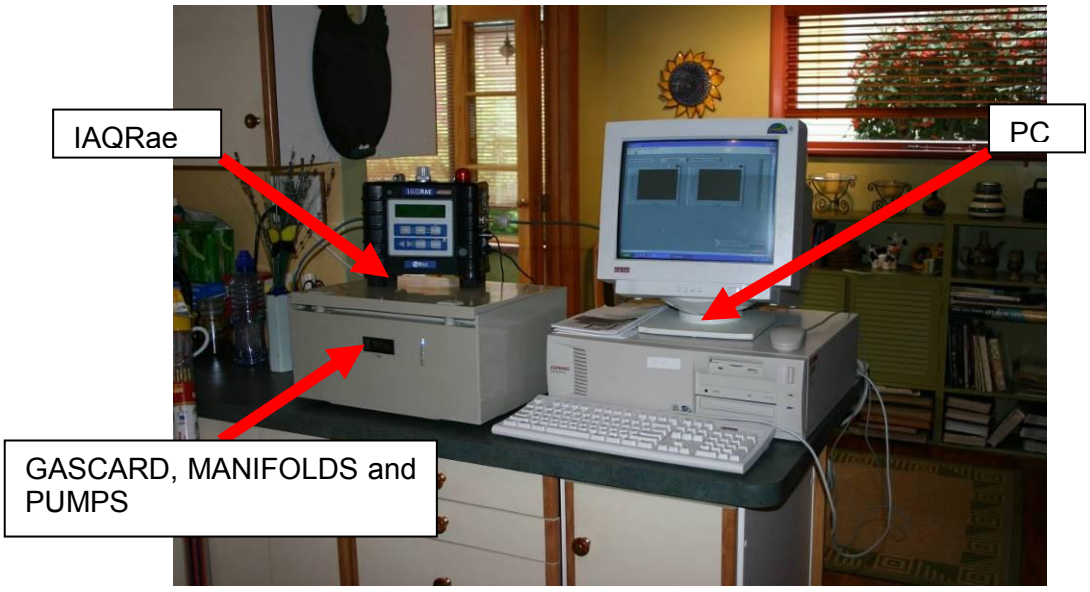

Figure 17. Picture of the air leakage apparatus and of the PC for data logging.

Figure 18. Pictures of part of the network of polyurethane tubes needed to inject tracer gases and draw air samples from different zones of the building.

Figure 19. Picture of the tracer gas cylinders located outside the building for safety reasons.

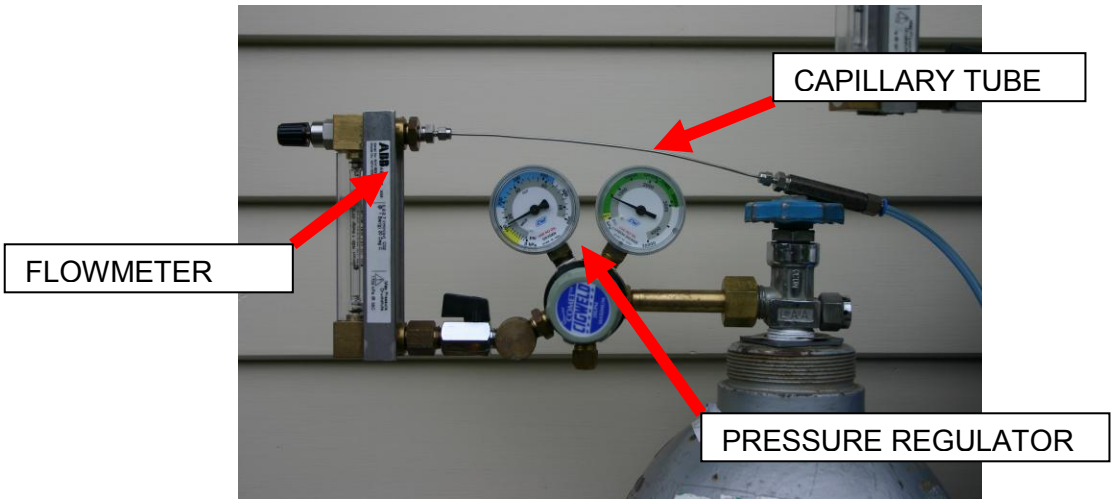

Figure 20. Pictures of the set-up used to dose tracer gas. A capillary tube reduces the flow rate to the range 0.1 – 1 l/min needed to perform the injection of tracer gas. The flow meter is also visible.

4.2 Dwelling in Silverstream (Upper Hutt)

The house monitored in Silverstream (Upper Hutt) is a one-storey house which has a pitched roof with roof space and corrugated iron as roof cladding. For this house, we concentrated on measuring air flow rates between the living space and outdoors, between the roof space and outdoors and between living space and roof space. To achieve this goal, we installed a network of tubes in the different rooms composing the living spaces and a network of tubes in the roof space and then injected a different tracer gas in each zone. The same kind of experiment was performed three times in order to have values of air flows under different climatic conditions. For each measurement we display six graphs:

- temperature in the living space, in the roof space and outdoors
- hourly vectorial averages of wind speed and direction
- concentration of tracer gas 1 in the living space and in the roof space
- concentration of tracer gas 2 in the living space and in the roof space
- calculated values of six air flow rates (two graphs).

We called outdoors Zone 0, the living space Zone 1 and the roof space Zone 2. With this identification of the zones, the six air flow rates are the same depicted on the right side of Figure 1, namely: Q_{10} is the air flow rate from living room to outdoors; Q_{01} from outdoors to living room; Q_{20} from roof space to outdoors; Q_{02} from outdoors to roof space; Q_{12} from living room to roof space; Q_{21} from roof space to living room.

The graphs for the three experiments are shown in the following series of figures:

- Figure 21 to Figure 26: measurement series 1
- Figure 27 to Figure 32: measurements series 2
- Figure 33 to Figure 38: measurement series 3.

The tracer gases used for all three experiments were CO_2 and N_2O. They were injected in the following way:

Measurement series 1	Zone 1 CO_2 at 0.5 l/min
	Zone 2 N_2O at 0.2 l/min
Measurement series 2	Zone 1 CO_2 at 0.6 l/min
	Zone 2 N_2O at 0.3 l/min
Measurement series 3	Zone 1 N_2O at 0.2 l/min
	Zone 2 CO_2 at 0.5 l/min

The records of temperatures show how the roof space become sensibly hotter than the outside air during the day but slightly cooler during the night. This effect is a consequence of the radiant cooling of the metallic cladding of the roof during the night (a comprehensive explanation is given in Paragraph 4.3).

A comparison of Figure 26, Figure 32 and Figure 38 shows how the air flow rates into and out of the roof space are strongly dependent on the wind speed. Theoretically, in the absence of the stack effect, the air flow rate is proportional the value of the pressure difference generated by the wind raised to the power of n (Hagentoft 2001, Liddamet 1986). If we assume a fully turbulent flow through the cracks of the roof, n is equal to 0.5. The pressure difference generated by the wind is proportional to the square of the average wind speed. So we have a linear dependency of the air flow rate with the average wind speed.

$$Q \propto \Delta p_{wind}^{0.5} \tag{4.1}$$

$$\Delta p_{wind} \propto \overline{U}_{wind}^{2} \tag{4.2}$$

$$Q \propto \overline{U}_{wind} \tag{4.3}$$

When the wind speed is around 2 m/s, Q_{02} and Q_{20} are about 150 m^3/h (see Figure 26). When the wind speed is around 1 m/s, Q_{02} and Q_{20} are about 75 m^3/h (see Figure 32). When the wind is absent, Q_{02} and Q_{20} are about 25 m^3/h (see Figure 38). This last value could be representative of the stack effect.

A comparison of Figure 25, Figure 31 and Figure 37 shows that a more complex interplay of factors is in action to explain the behaviour of the air flow rates Q_{21}, Q_{21}, Q_{01} and Q_{10}. When the wind speeds are 2 m/s, 1 m/s and 0 m/s, Q_{21} decreases (15 m^3/h, 5 m^3/h and 2.5 m^3/h) while Q_{21} increases (5 m^3/h, 7.5 m^3/h and 12.5 m^3/h). When the wind is stronger, there is a net air flow going from the roof to the living space but when the wind is absent there is a net air flow from the living room to the roof space probably due to the temperature difference (around 7–8°C) between living space and roof space. When the wind speeds are 2 m/s, 1 m/s and 0 m/s, Q_{01} stays more or less constant (10 m^3/h, 15 m^3/h and 15 m^3/h) while Q_{01} decreases (20 m^3/s, 10 m^3/s and 5 m^3/s). When the wind is stronger, there is a greater air flow going from the living space towards outside but the air flow coming into the living space from the outside seems to stay constant.

4.3 Dwelling in Whitby (Porirua)

The house we monitored in Whitby (Porirua) is a one-storey house which has a pitched roof with roof space and corrugated iron as roof cladding. For this house, we concentrated on studying the relation between roof space and the cavity between underlay and roof cladding. To achieve this goal, we installed a network of tubes in the roof space and a system of tubes provided with needles for the cavity. Injecting tracer gas in the cavity underlay-cladding presents some challenges because there is no direct access to the cavity from the roof space. In order to overcome this problem we installed needles at the end of the polyurethane tubes and inserted these needles through the underlay in order to inject and draw air samples from the cavity. We injected N_2O at a rate of 0.2 l/min in the roof space and CO_2 at a rate of 0.5 l/min in the cavity underlay-cladding. For this measurement we display four graphs:

- temperature in the living space, in the roof space, outdoors and under the cladding
- hourly vectorial averages of wind speed and direction
- concentration of tracer gas 1 in the roof space and in the cavity
- concentration of tracer gas 2 in the roof space and in the cavity.

In this house, besides the BRANZ temperature loggers described previously, we also used a special temperature logger able to record type T thermocouple measurements. This set-up is more suitable in order to measure temperatures in confined spaces. We installed some type T thermocouples on the bottom side of the roof cladding near the gutter on the north facing slope of the roof. This slope is the same as the one of the cavity underlay-cladding where we have injected the tracer gas. Figure 41 shows the behaviour of the different temperature recorded. This shows that during the night between day 2 and day 3 the temperature of the roof was slightly higher than the temperature of the outside air, but during the night between day 3 and day 4 the temperature of the roof dropped below the outside temperature.

During the same two nights, the temperature of the cladding was in the first case similar to the temperature of the outside air but in the second case was considerably lower, as a consequence dragging the temperature of the air in the roof down. Looking at Figure 42, we noticed that the night between day 2 and day 3 was quite windy (and probably cloudy), so the radiative cooling of the roof cladding was not active. But during the night between day 3 and day 4, the wind dropped (and the sky was probably clear and starry) allowing the radiative cooling of the roof cladding to be very efficient and making the temperature of the roof cladding and of the roof space drop below the temperature of outside air. This kind of behaviour is of paramount importance for the study of the properties of building underlays because they influence the process of moisture formation and removal in the roof space. As a side note, the temperature of the cladding varies more wildly than the other temperatures. This is more evident during daytime. These rapid variations are probably due to the passage of clouds which screen the sun. Direct sunlight heats up the cladding quickly while cloudy periods cool down the cladding.

Figures 43 and 44 show the temporal behaviour of the concentration of tracer gases. The concentrations behave in a similar fashion and they display peaks and troughs at the same times. The concentration is higher when the wind is absent, allowing the tracer gas to accumulate. When the wind is present, it increases the air flows in the zones and the concentrations drop. The concentration of N_2O is similar in the roof space (where it was injected) and in the cavity underlay-cladding. This seems to imply that the cavity is connected quite efficiently with the roof space. This is confirmed by

the behaviour of the concentration of CO_2 (injected in the cavity) during day 3 when the wind was nearly absent. In that case, the concentrations were very similar.

Due to this close connection between roof space and cavity, the calculation of air flows becomes meaningless. When the different concentrations and source terms are introduced in the linear system of equations (2.12) and (2.13), the resulting values of air flow rates are very high. Mathematically this is due to the fact that the linear system gets very close to become singular, physically to the fact that the two cavities are closely connected.

4.4 Dwelling in Raumati South (Raumati)

The house we monitored in Raumati South (Raumati) is a one-storey house which has a pitched roof with roof space and metallic tiles as roof cladding. For this house, we concentrated on studying air flows in the cavity between underlay and cladding. To achieve this, we set up a network of polyurethane tubes with needles at their ends and inserted these needles through the underlay in order to inject and draw air samples from the cavity. We studied a section of the cavity located on the northern slope of the roof injecting two tracer gases, one at the top of the cavity near the ridge (N_2O) and another at the bottom of the cavity near the eaves (CO_2). The aim of this experimental set-up was to probe the direction of the flow of air in the cavity under different climatic conditions. If there is a downward air flow, the concentration of N_2O should increase at the bottom of the cavity. If there is an upward air flow, the concentration of CO_2 should increase at the top of the cavity. In reality the interpretation of the experimental results is made more complex by the fact that N_2O has a density of 1.87 kg/m3 and CO_2 of 1.98 kg/m3, which is about 1.5 times the density of air. In the absence of any air flow, the two tracer gases tend to go downward due to purely gravitational effects.

For this measurement we display three graphs:

- hourly vectorial averages of wind speed and direction
- concentration of tracer gas 1 and 2 at the top and at the bottom of the cavity
- temperature in different location of the roof space, of the cladding and outdoors.

In Figure 46 we report the concentration of N_2O and of CO_2 at the top and at the bottom of the cavity. In two periods, indicated by a blue arrow, the concentration of CO_2 in the two locations is equal and similar to the background concentration of CO_2 (around 500 ppm). On the contrary, the concentration of N_2O decreased considerably near the top of the cavity and increased near the bottom of the cavity. This leads us to infer that during these periods there was no air flow or a downward air flow because CO_2 wasn't carried up the cavity and didn't accumulate any more near the bottom of the cavity, and simultaneously N_2O was quite efficiently carried down the cavity and didn't accumulate any more near the top of the cavity. These two periods corresponds to times when the wind was absent.

Something quite different happens when the wind is present. During the first period indicated by an orange arrow, the concentration of CO_2 near the bottom of the cavity and the concentration of N_2O near the top of the cavity suddenly increase considerably. This seems to hint to the presence of an upward flow which contrasts the natural tendency of the two gases to drift downwards and leads to a pile-up of the two gases near the zones where they are injected. During the second period indicated by an orange arrow, the concentration of CO_2 near the bottom of the cavity and the concentration of N_2O near the top of the cavity at first suddenly increase considerably but then they decrease, reproducing a pattern similar to the ones of the periods indicated by the blue arrows. This seems to hint to the presence at first of an upward flow which contrasts the natural tendency of the two gases to drift downwards and

leads to a pile-up of the two gases near the zones where they are injected, but later it hints to the presence of a downward air flow.

A possible explanation for this change of behaviour can be sought in the profile of pressure generated on the roof by the wind. Figure 48 (left side because the house under examination has a low pitched roof) shows an example of pressure distribution (Liddamet 1986). The pressure is always negative, that is to say, the impinging wind generates suction on the cladding of the roof. If we assume that the air moves from the point of low suction to the point of high suction, we have an air flow from eaves to ridge ($\alpha \rightarrow \beta$) and from ridge to eaves ($\gamma \rightarrow \delta$). This air movement is opposite to the direction of the wind. We can then apply this consideration to the interpretation of the experimental results. During the first windy period, we have a southerly wind which should generate an upward flow in the northern cavity. During the second windy period, we have at the beginning a southerly wind (generating an upward flow in the northern cavity) which suddenly changes to a stronger northerly wind (generating a downward flow in the northern cavity).

5. CONCLUSIONS

We have reported the successful implementation of the constant concentration multi-tracer gas method applied to the study of air flow patterns in roofs of residential dwellings. A stand-alone apparatus and dedicated software have been designed and developed. This system has been deployed in private dwellings where several kinds of measurements of air flows have been taken. At the same time climatic conditions have been monitored.

The analysis of the experimental results has enlightened the complexity of the task of measuring air flows in roof spaces with the aim of studying building underlays. Despite this complexity, a reasonable agreement has been found between the behaviour of climatic data (the physical drivers of the physical process) and the magnitude of air flow rates in the roof.

These field measurements have provided a useful set of data and an invaluable experience to guide the study of building underlay to be carried out in the experimental test building.

6. REFERENCES

Hagentoft C-E. 2001. Introduction to building physics. Studentlitteratur, Lund, Sweden.

Liddament M W. 1986. Air Infiltration Calculation Techniques – An applications Guide. AIVC, Bracknell, United Kingdom.

Roulet C-A and Compagnon R. 1989. 'Multizone Tracer Gas Infiltration Measurements – Interpretation Algorithms for Non-Isothermal Case'. *Building and Environment* 24(3): 221–227.

Sandberg M and Stymne H. 1989. 'The Constant Tracer Flow Technique'. *Building and Environment* 24(3): 209–219.

Trechsel H R, editor. 1994. Manual on Moisture Control in Buildings (ASTM manual series: MNL 18). ASTM, Philadelphia, United States of America.

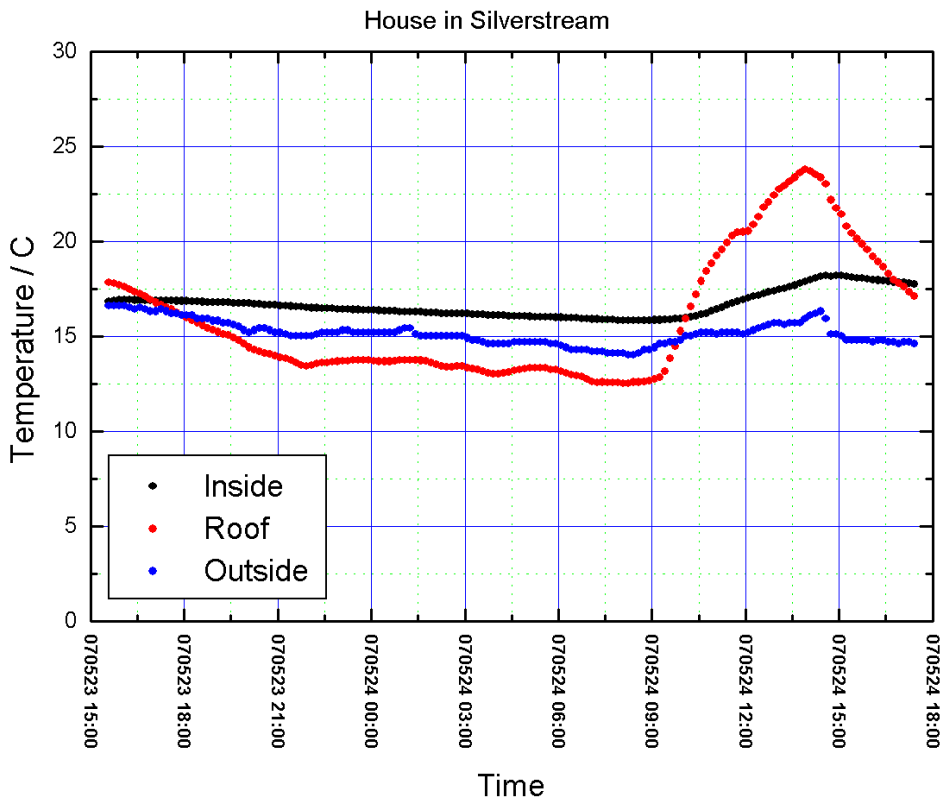

Figure 21. Temperatures in the living space, in the roof space and outdoors.

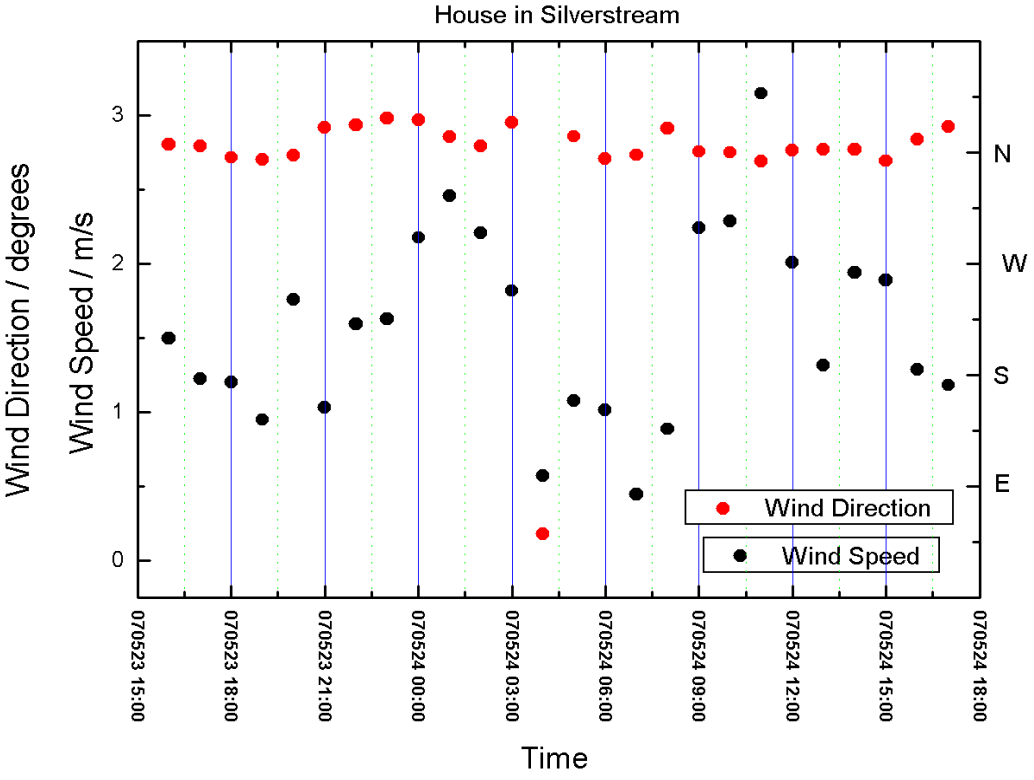

Figure 22. Hourly averages of wind speed and direction.

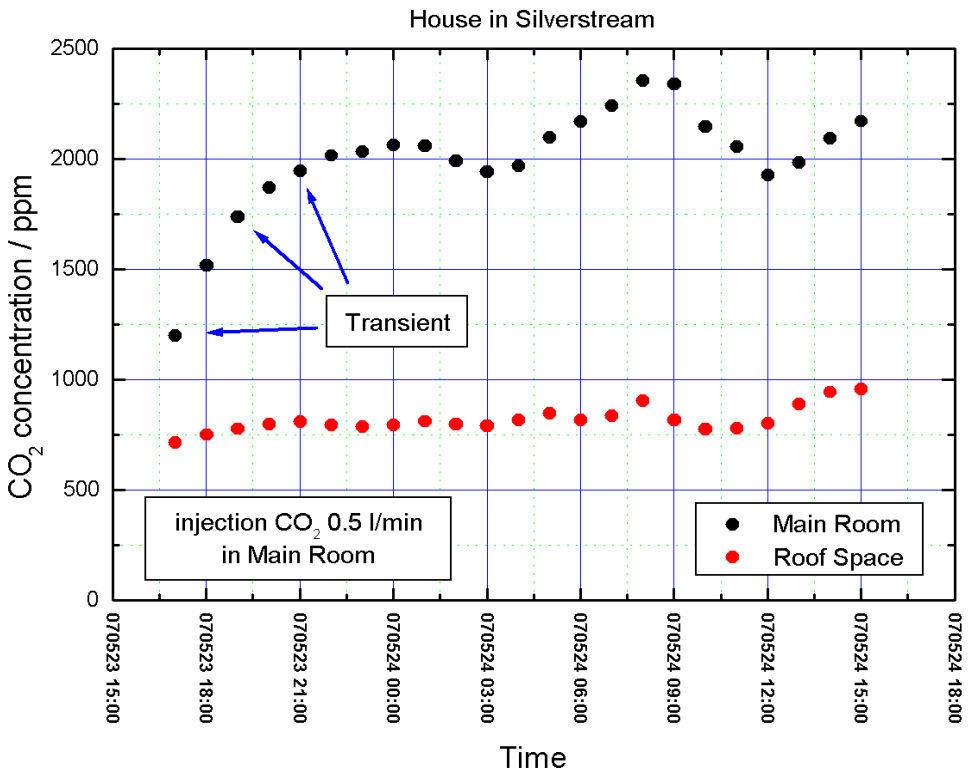

Figure 23. Temporal behaviour of the concentration of CO_2 which was injected in the living space of the house.

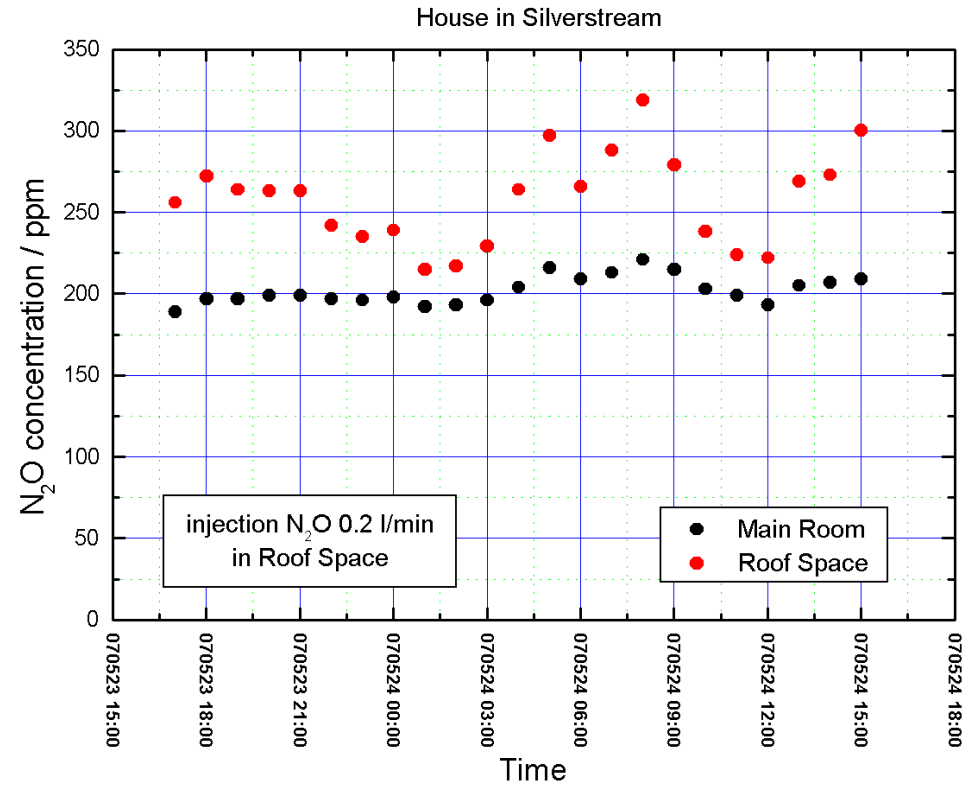

Figure 24. Temporal behaviour of the concentration of N_2O which was injected in the roof space of the house.

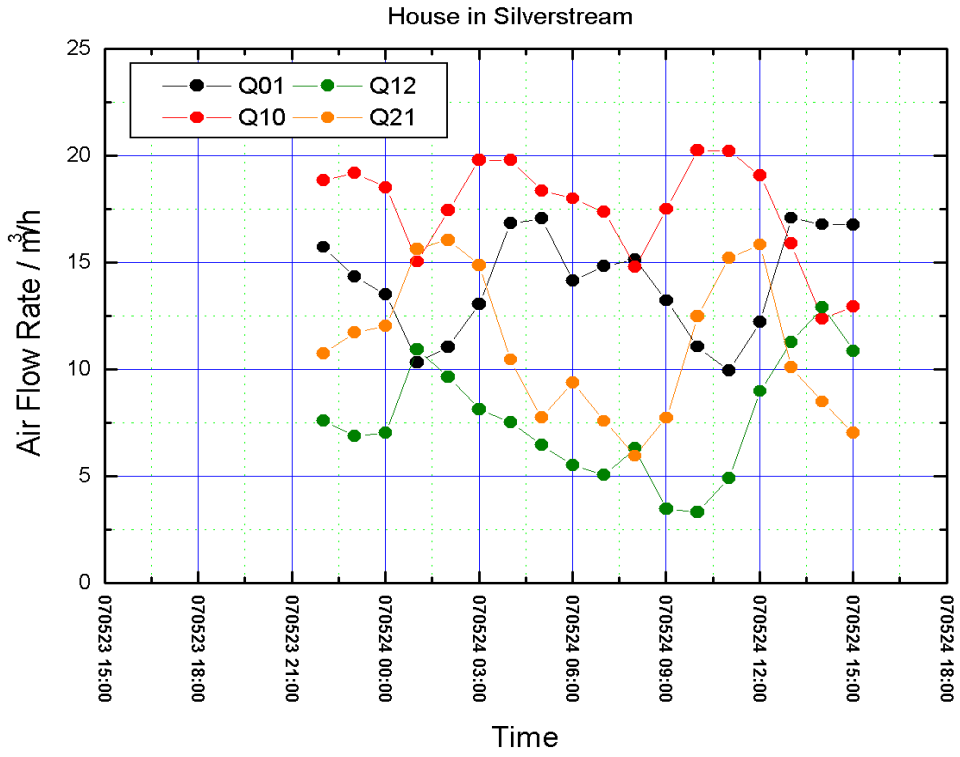

Figure 25. Calculated air flow rates. Q_{ij} indicates the rate of the air flow from zone i to zone j with 0=outdoors, 1=living space and 2=roof space.

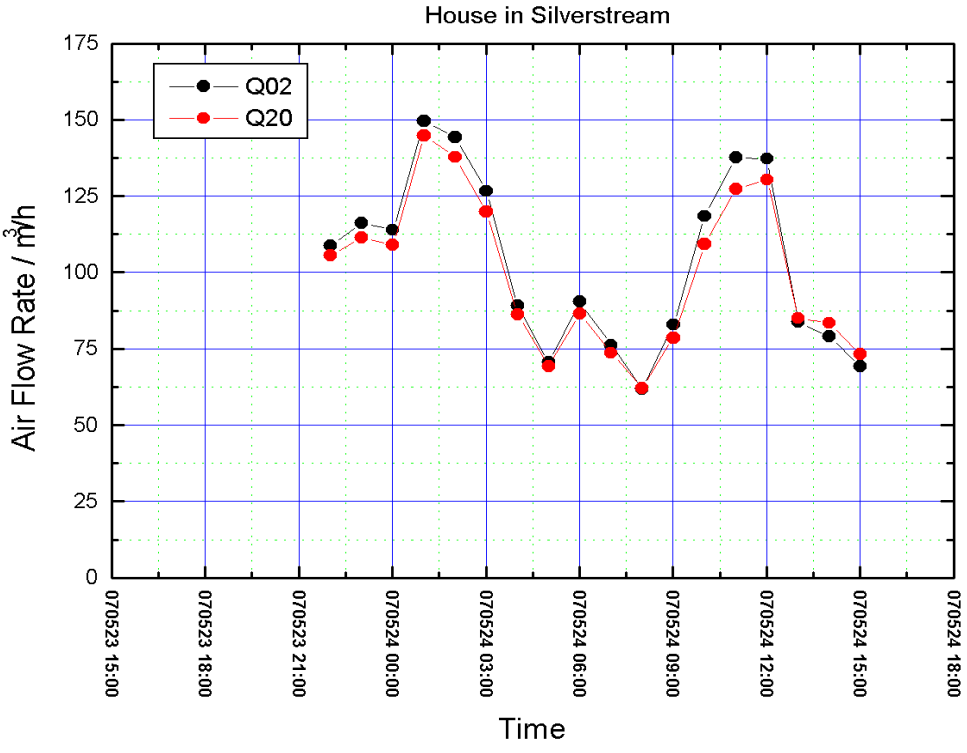

Figure 26. Calculated air flow rates. Q_{ij} indicates the rate of the air flow from zone i to zone j with 0=outdoors, 1=living space and 2=roof space.

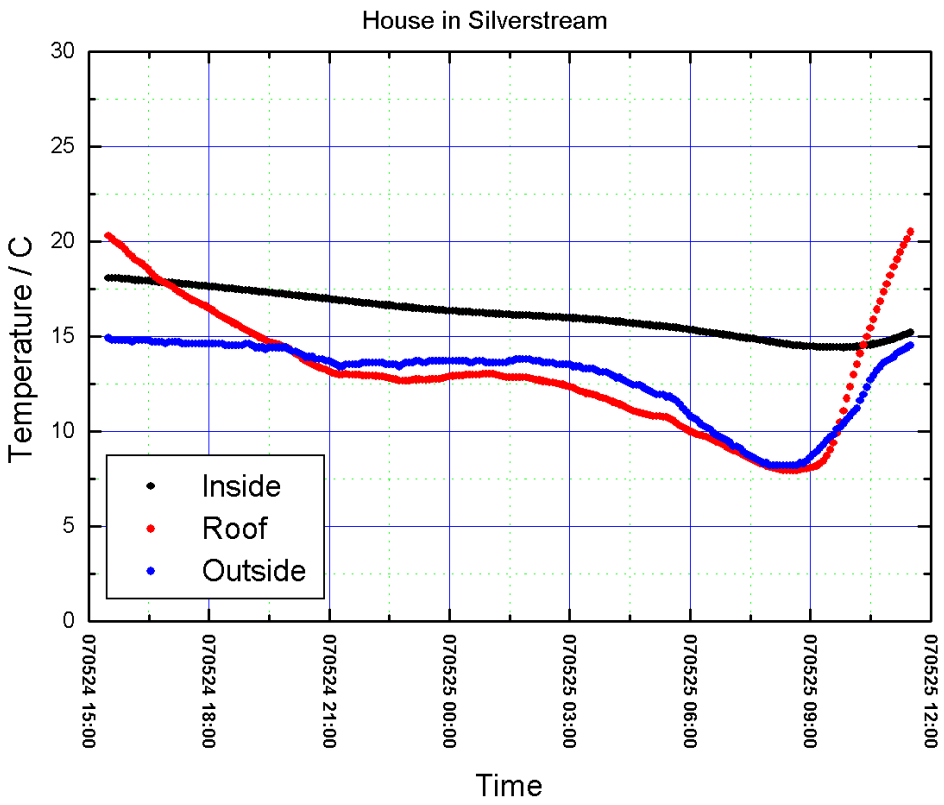

Figure 27. Temperatures in the living space, in the roof space and outdoors.

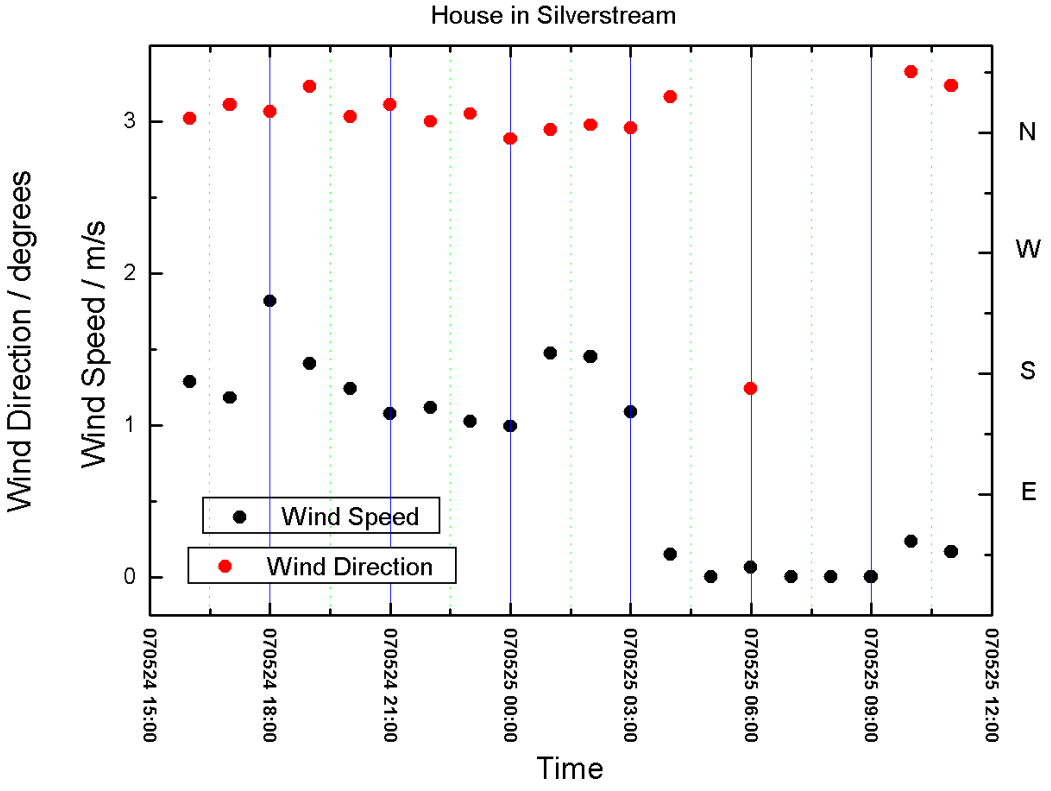

Figure 28. Hourly averages of wind speed and direction.

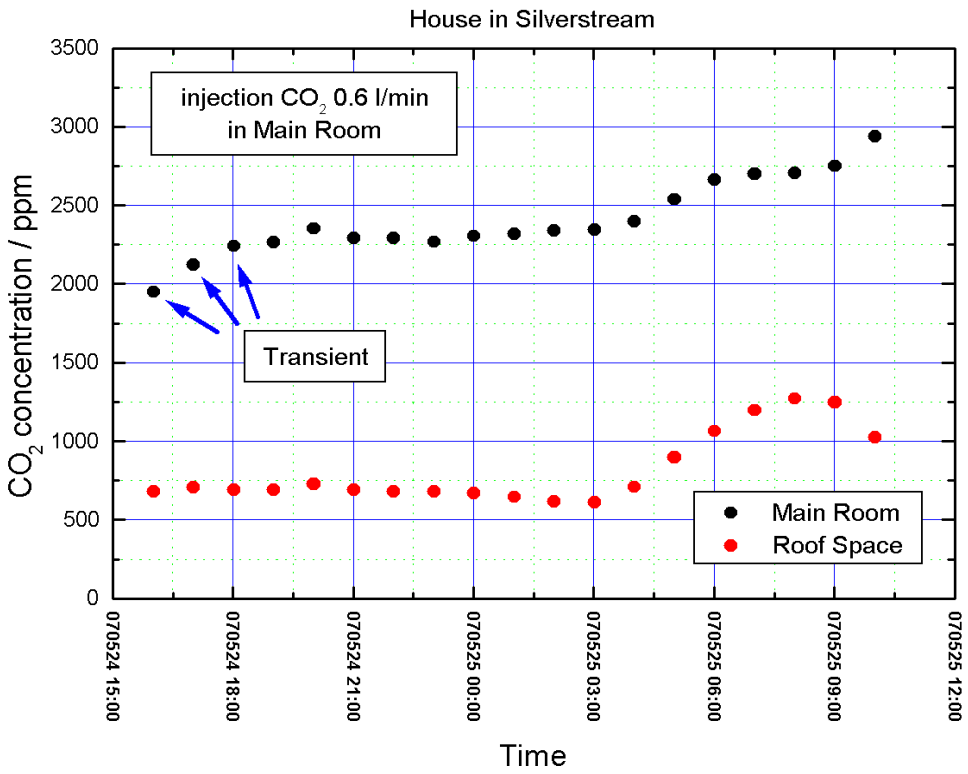

Figure 29. Temporal behaviour of the concentration of CO_2 which was injected in the living space of the house.

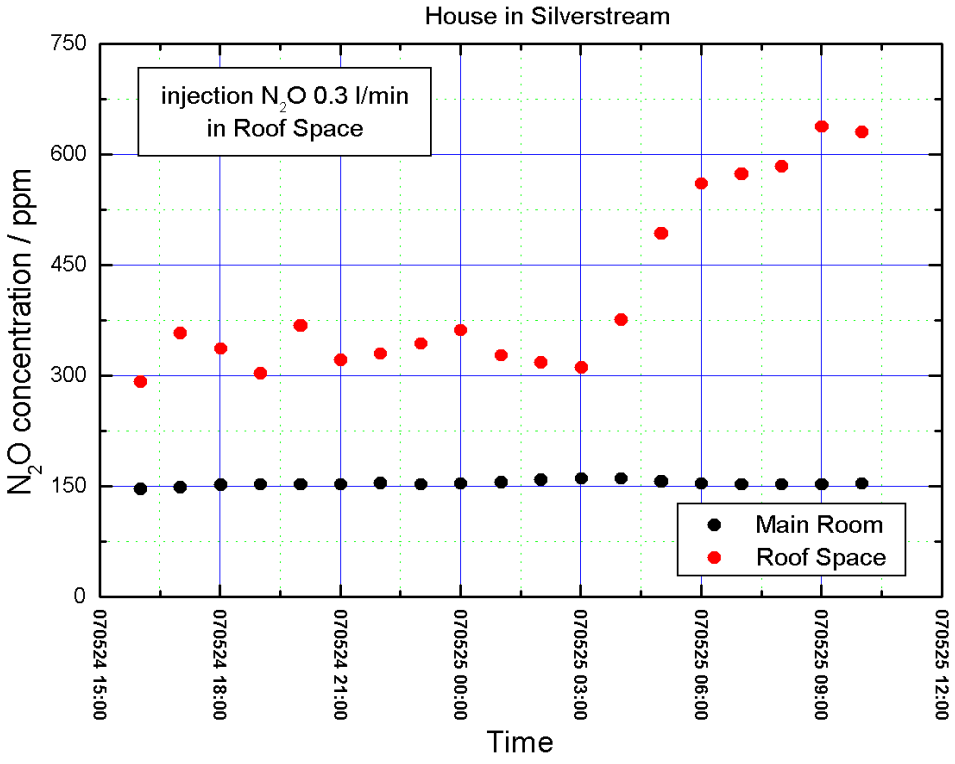

Figure 30. Temporal behaviour of the concentration of N_2O which was injected in the roof space of the house.

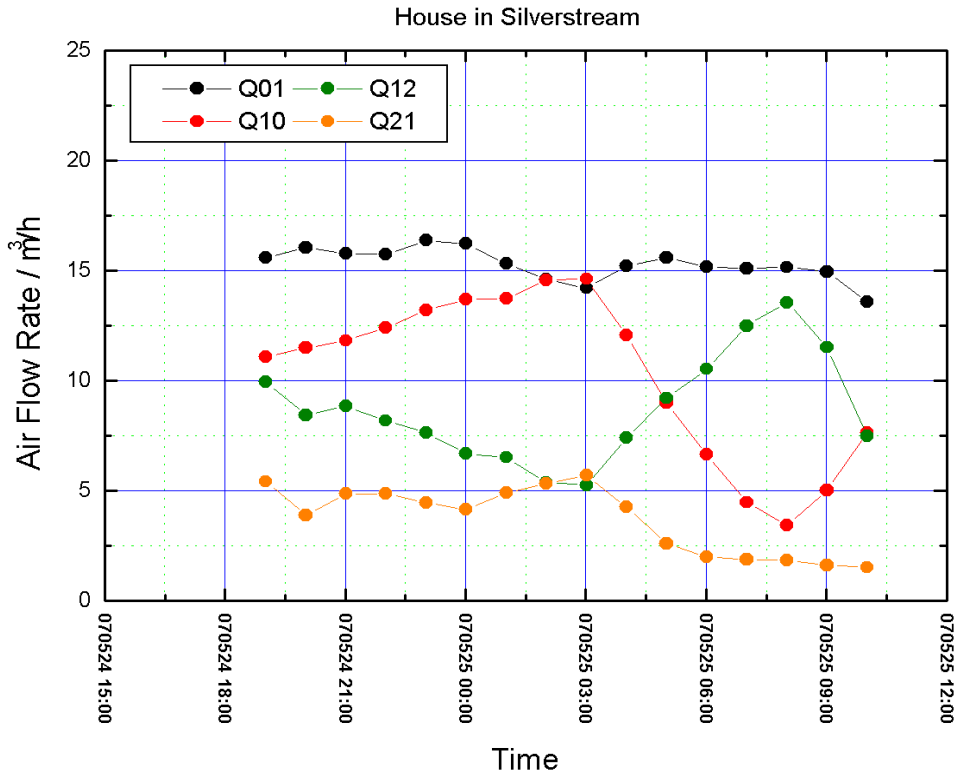

Figure 31. Calculated air flow rates. Q_{ij} indicates the rate of the air flow from zone i to zone j with 0=outdoors, 1=living space and 2=roof space.

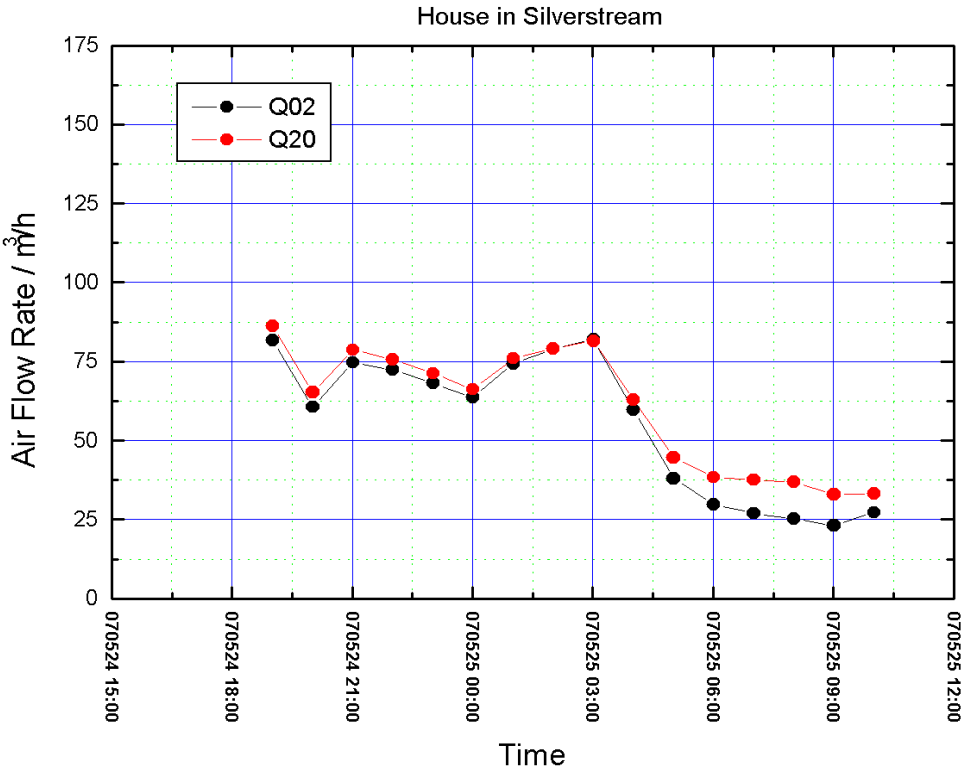

Figure 32. Calculated air flow rates. Q_{ij} indicates the rate of the air flow from zone i to zone j with 0=outdoors, 1=living space and 2=roof space.

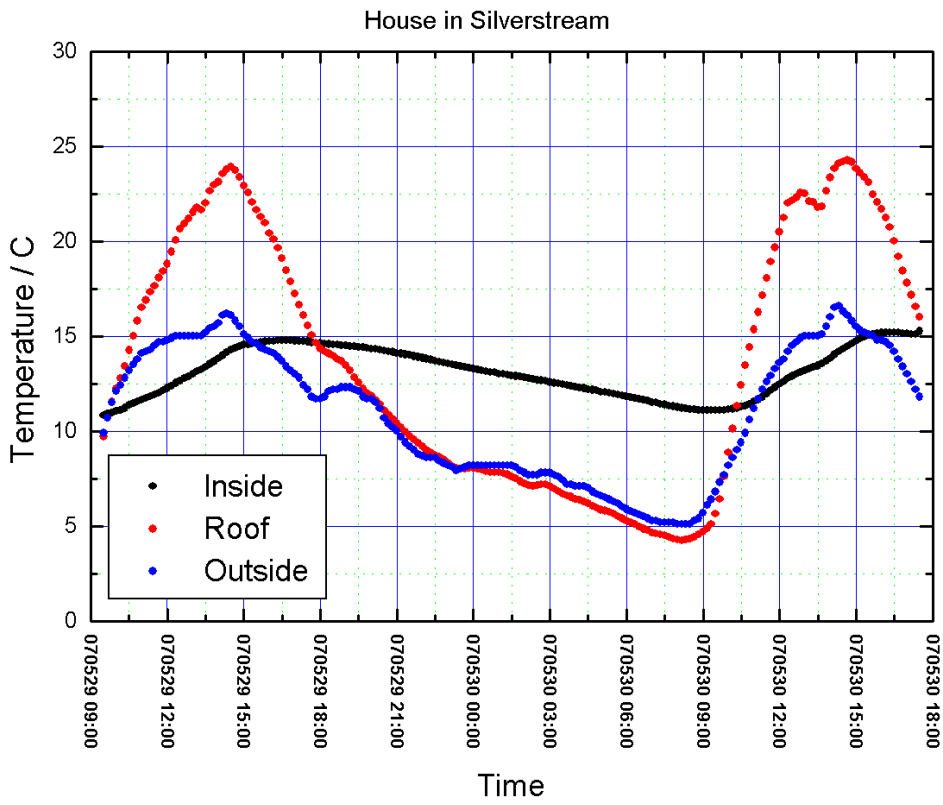

Figure 33. Temperatures in the living space, in the roof space and outdoors.

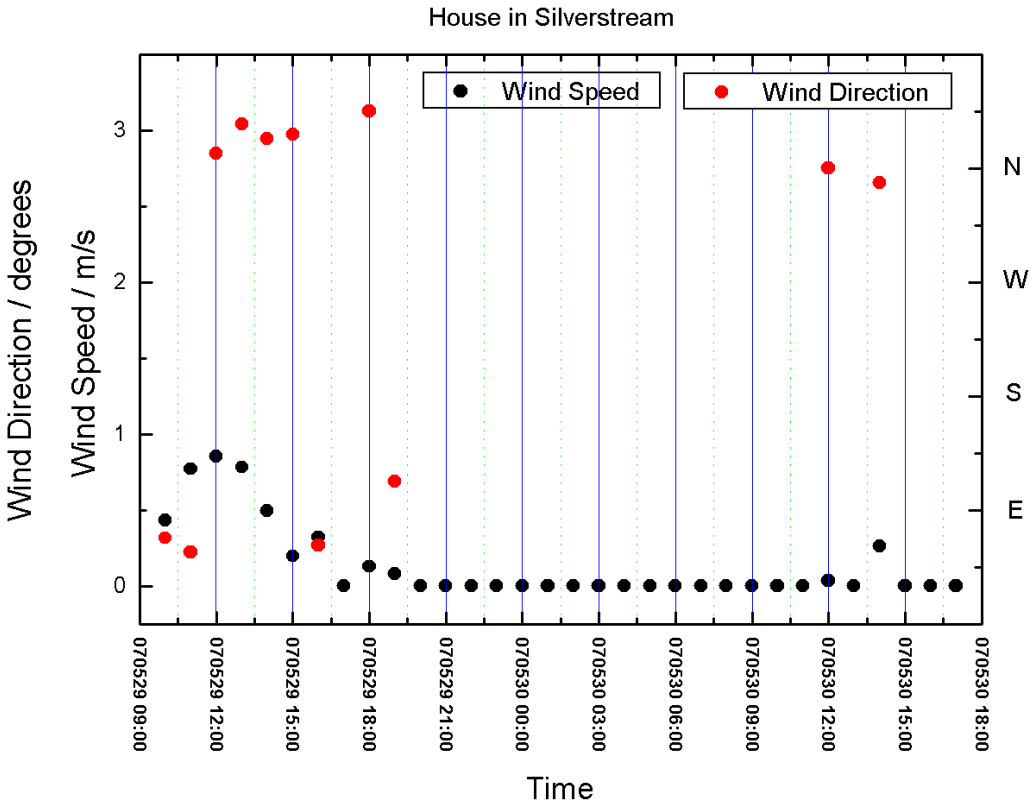

Figure 34. Hourly averages of wind speed and direction.

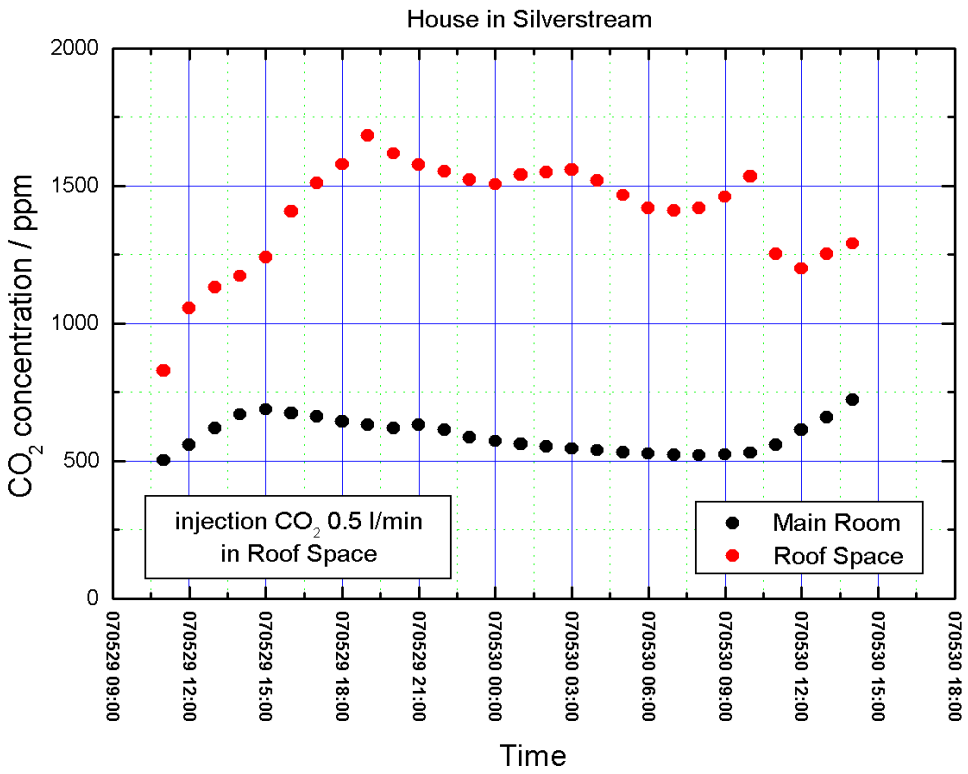

Figure 35. Temporal behaviour of the concentration of CO_2 which was injected in the roof space of the house.

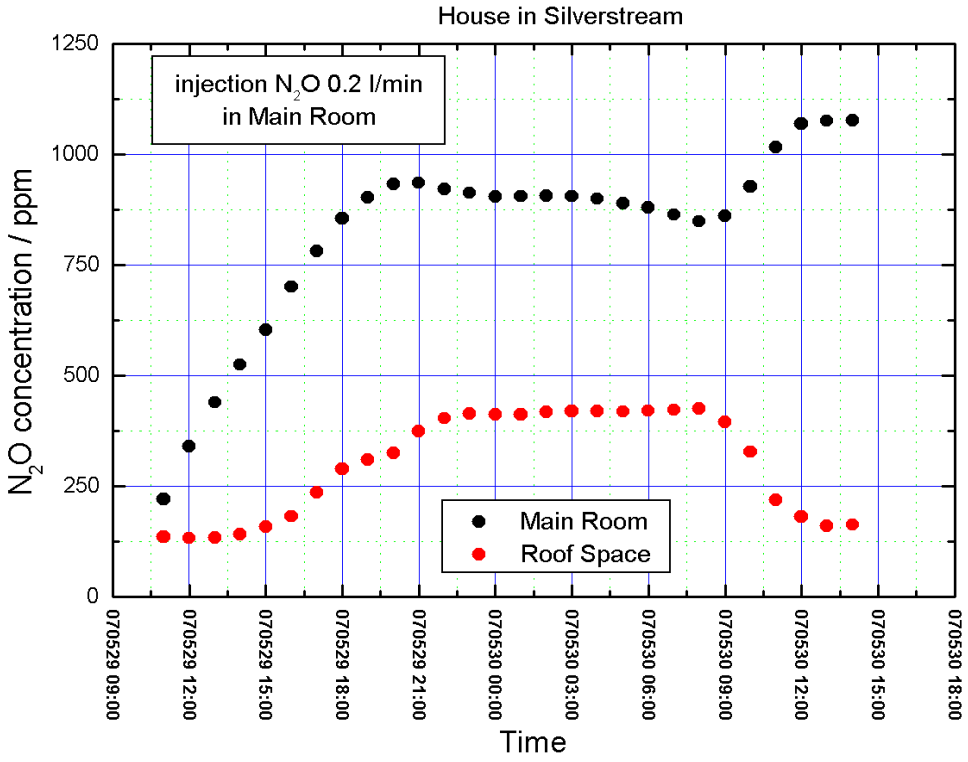

Figure 36. Temporal behaviour of the concentration of N_2O which was injected in the living space of the house.

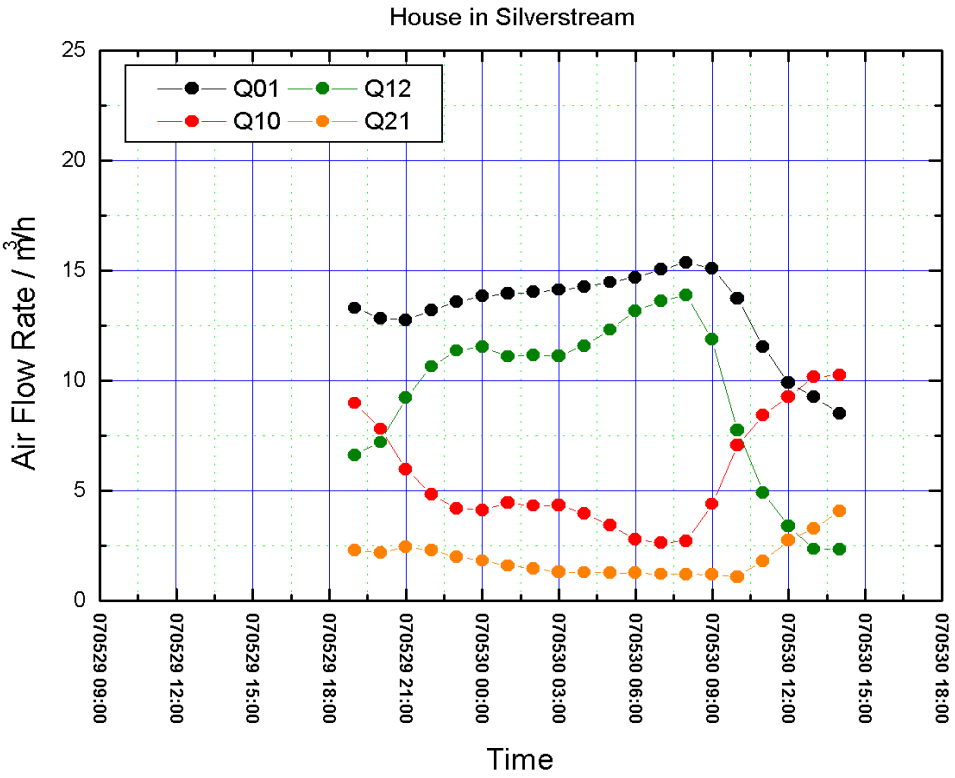

Figure 37. Calculated air flow rates. Q_{ij} indicates the rate of the air flow from zone i to zone j with 0=outdoors, 1=living space and 2=roof space.

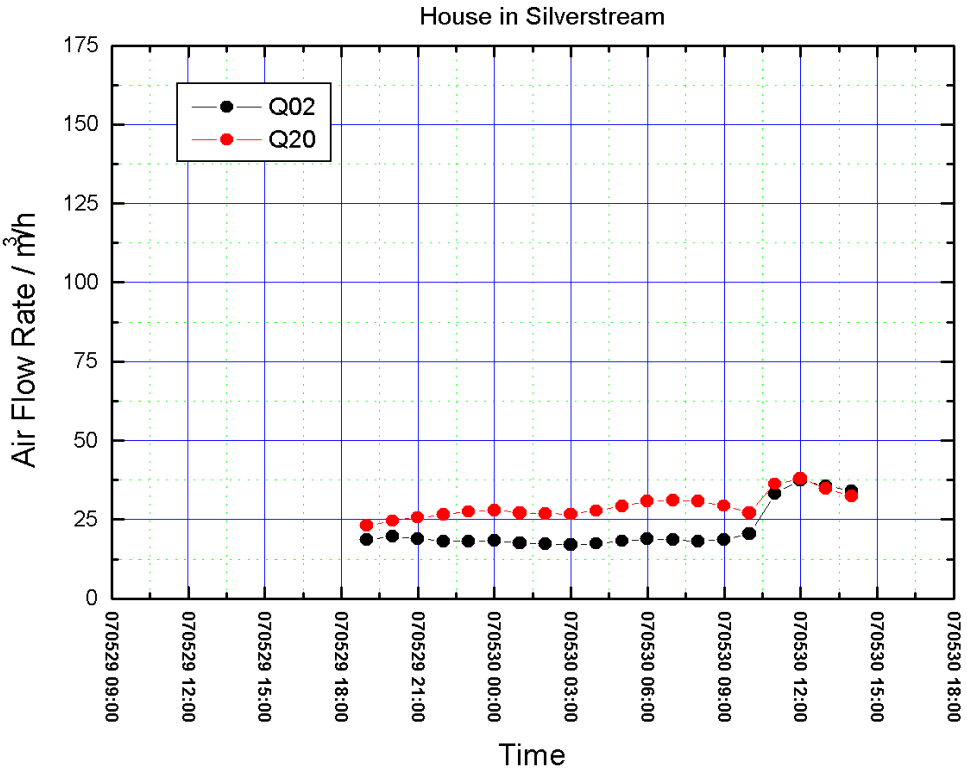

Figure 38. Calculated air flow rates. Q_{ij} indicates the rate of the air flow from zone i to zone j with 0=outdoors, 1=living space and 2=roof space.

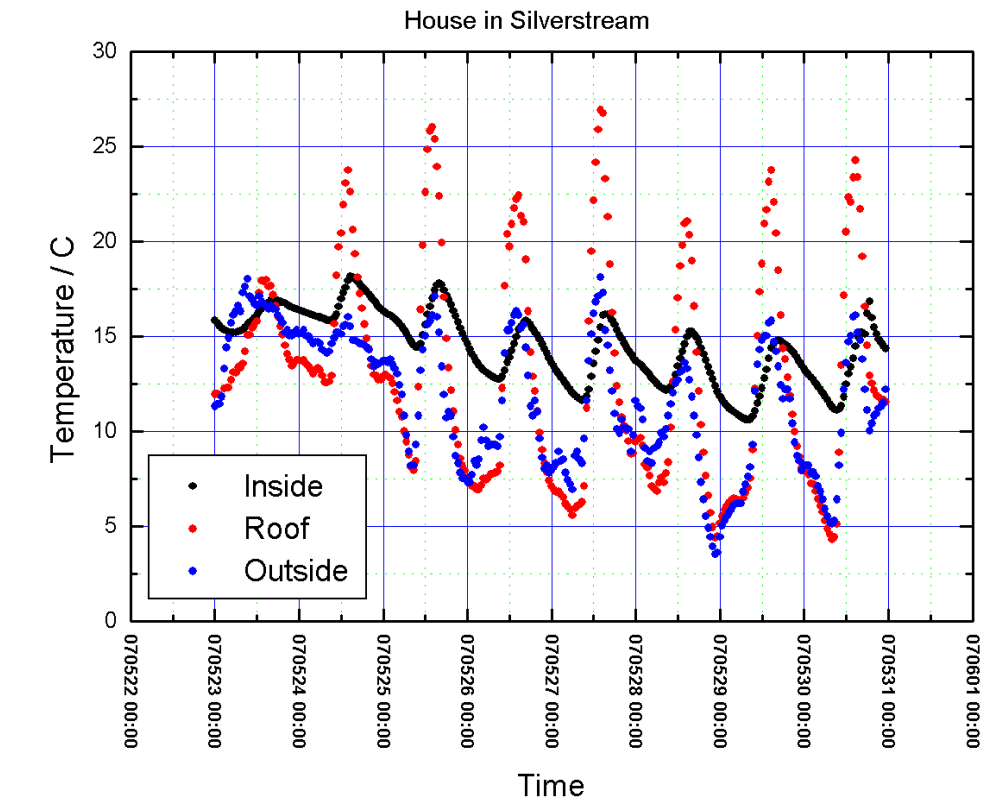

Figure 39. Temperatures in the living space, in the roof space and outdoors.

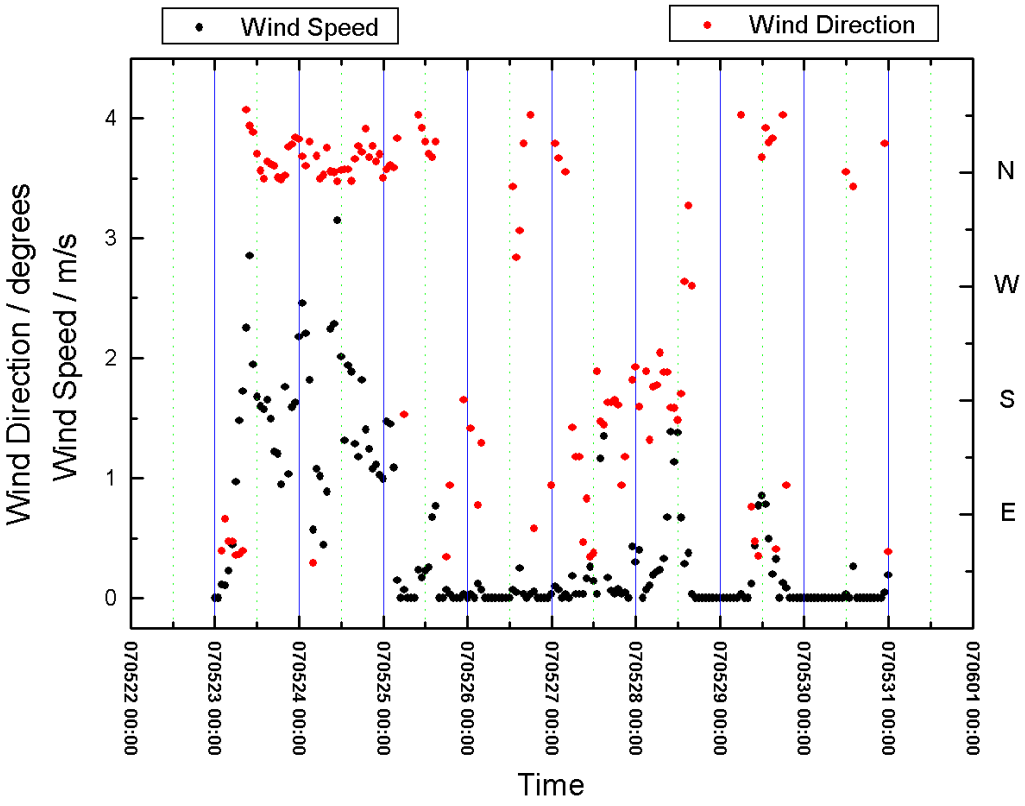

Figure 40. Hourly averages of wind speed and direction.

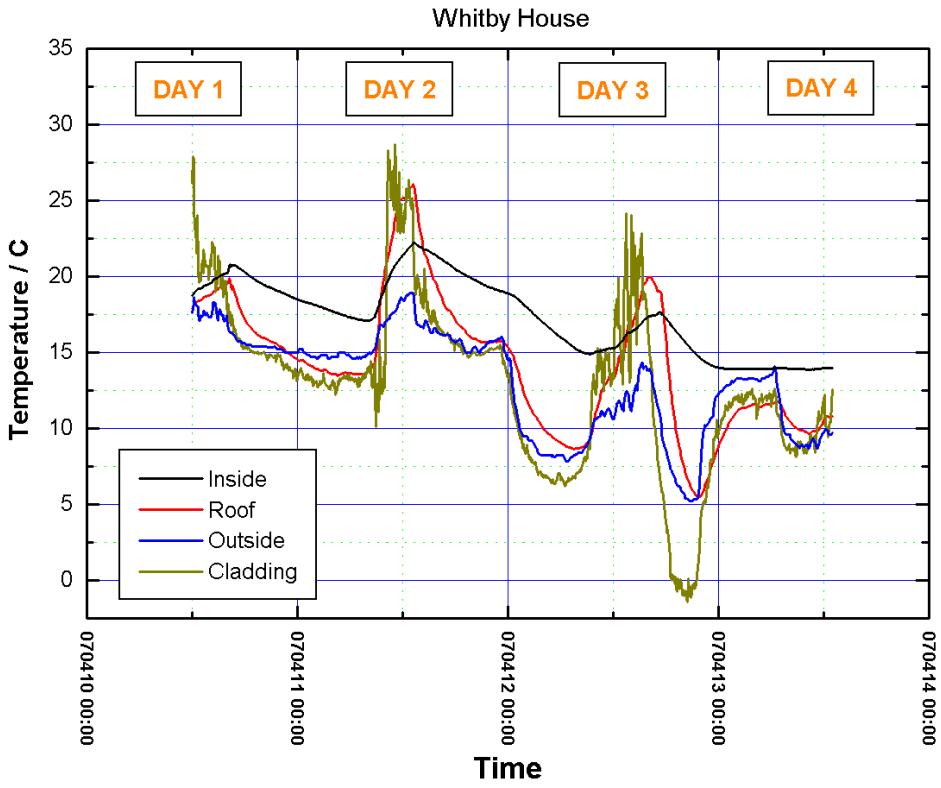

Figure 41. Temperatures in the living space, in the roof space, outdoors and of the cladding.

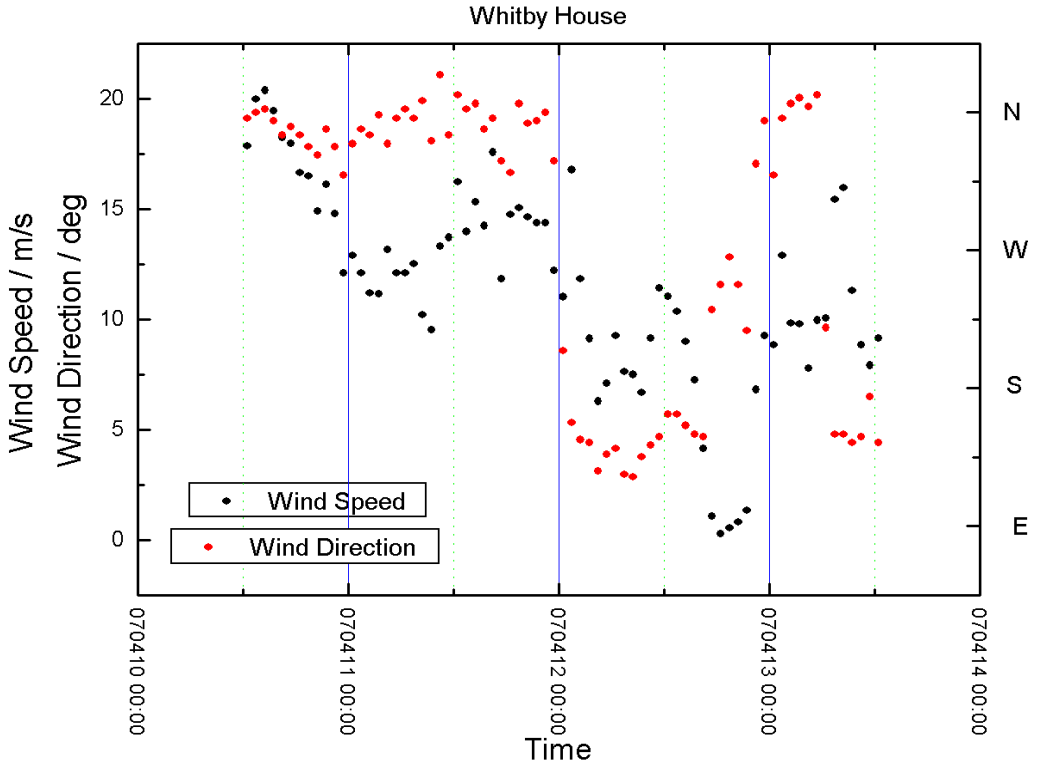

Figure 42. Hourly averages of wind speed and direction.

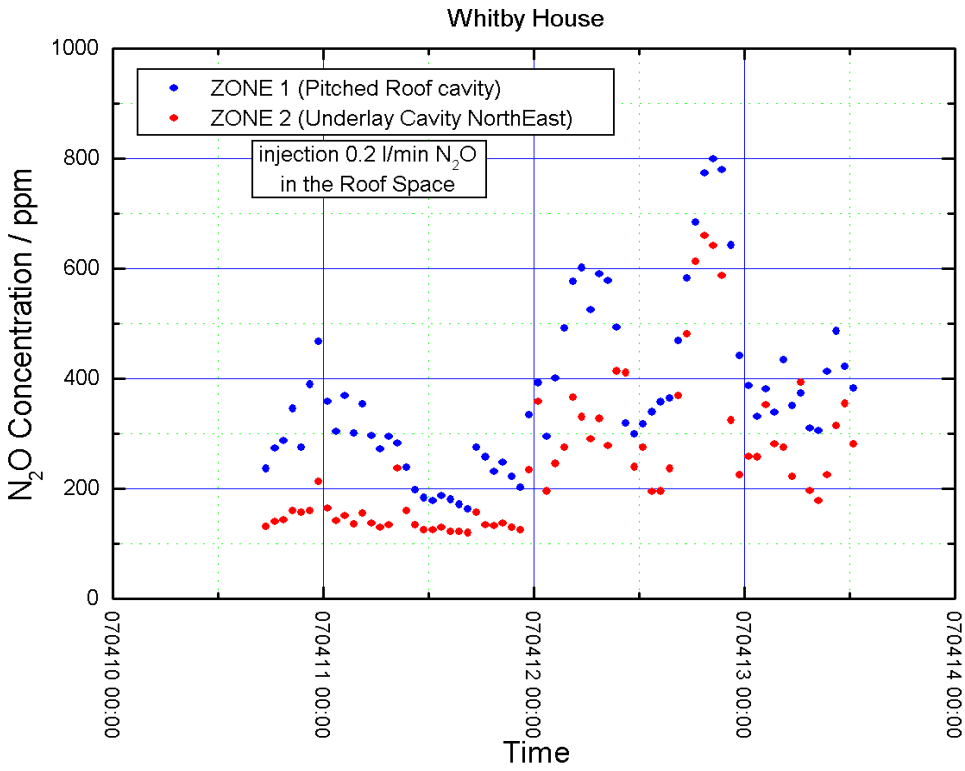

Figure 43. Temporal behaviour of the concentration of N_2O which was injected in the roof space of the house.

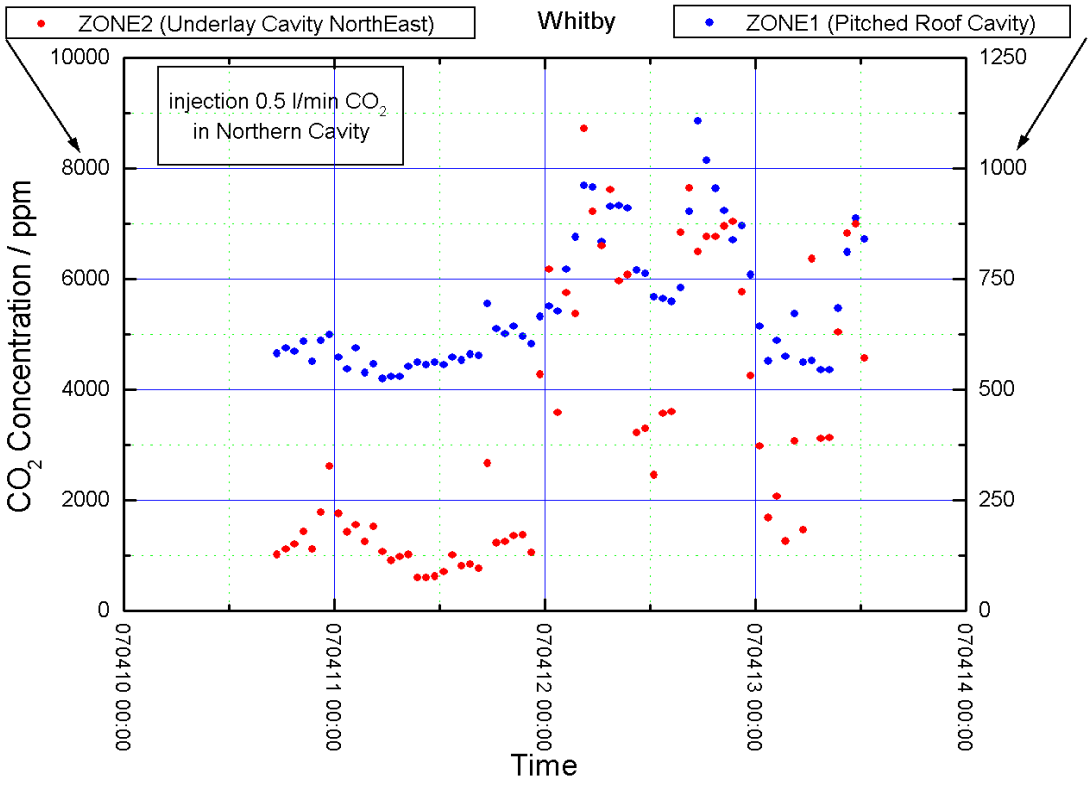

Figure 44. Temporal behaviour of the concentration of CO_2 which was injected in the northern cavity between underlay and cladding.

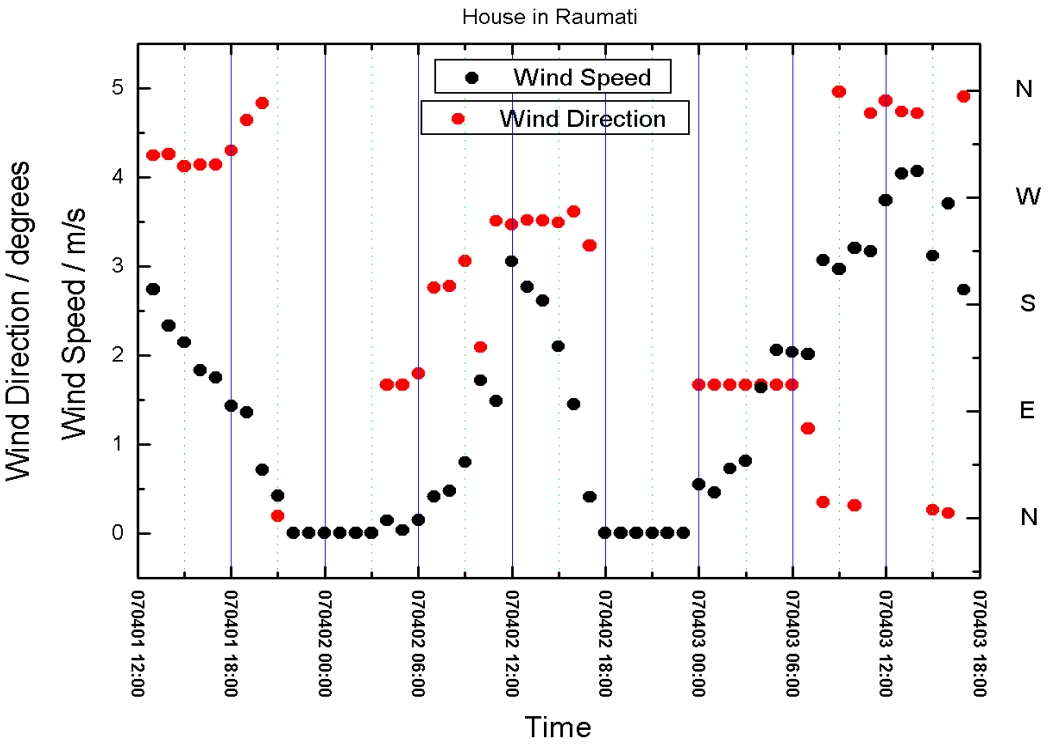

Figure 45. Hourly averages of wind speed and direction.

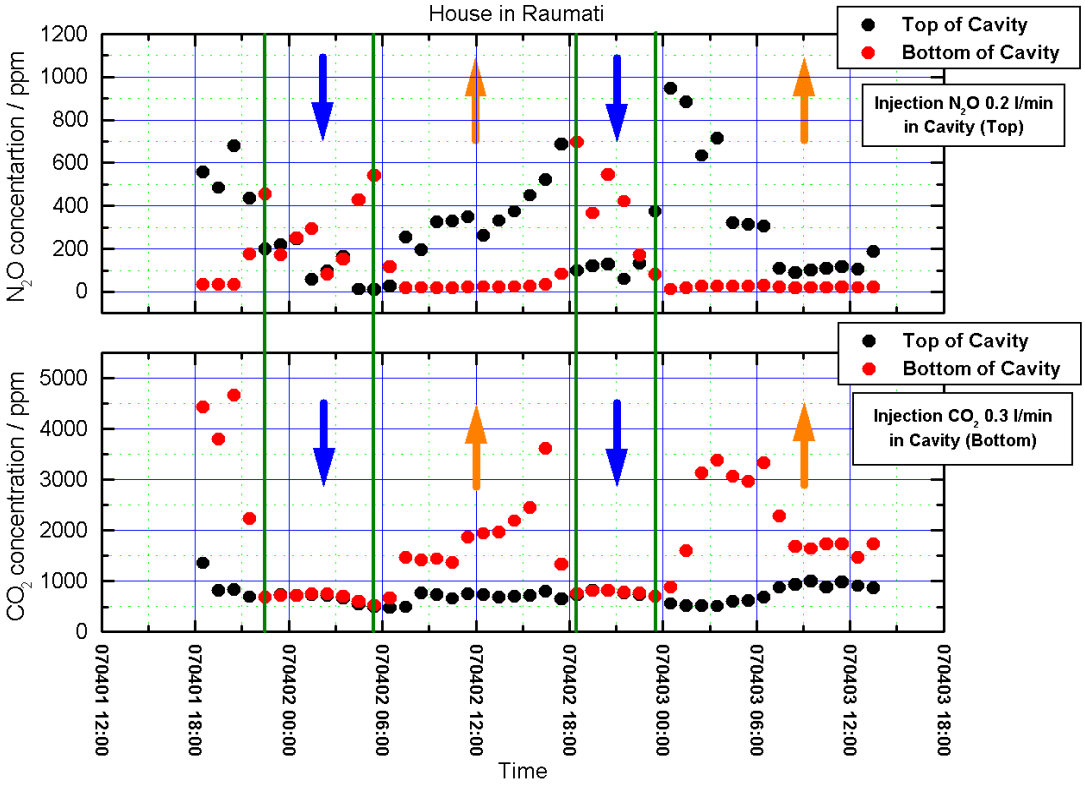

Figure 46. Temporal behaviour of the concentration of N_2O (above) and CO_2 (below). N_2O was injected at the top of the cavity underlay-cladding, CO_2 at the bottom of the cavity underlay-cladding.

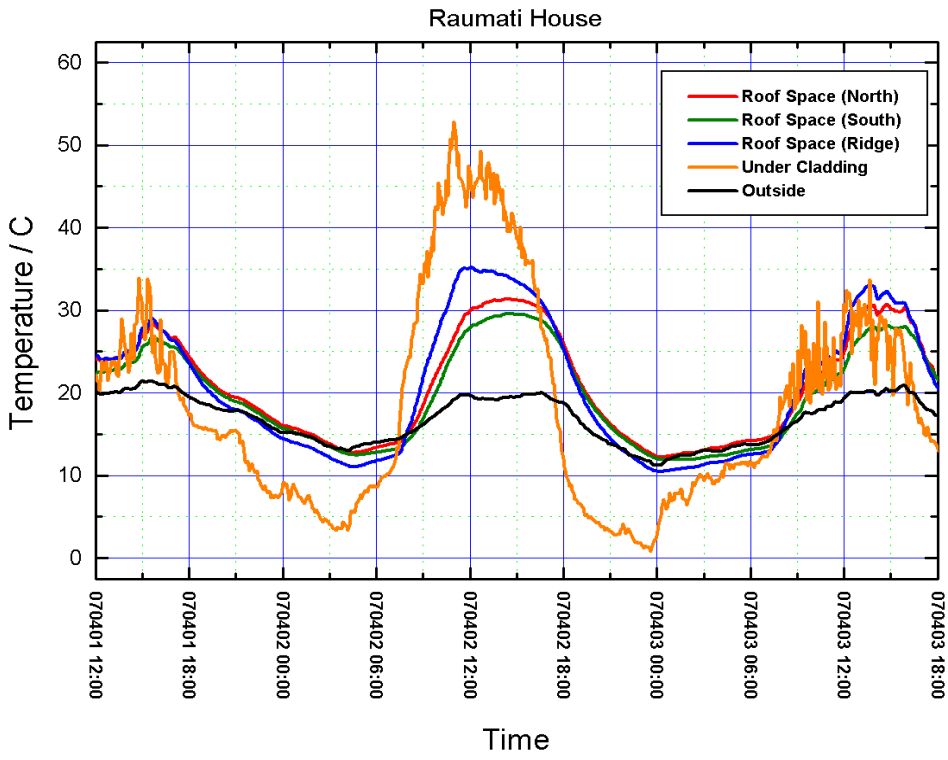

Figure 47. Temperatures in the roof space (northern side, southern side and near ridge), under the cladding and outdoors.

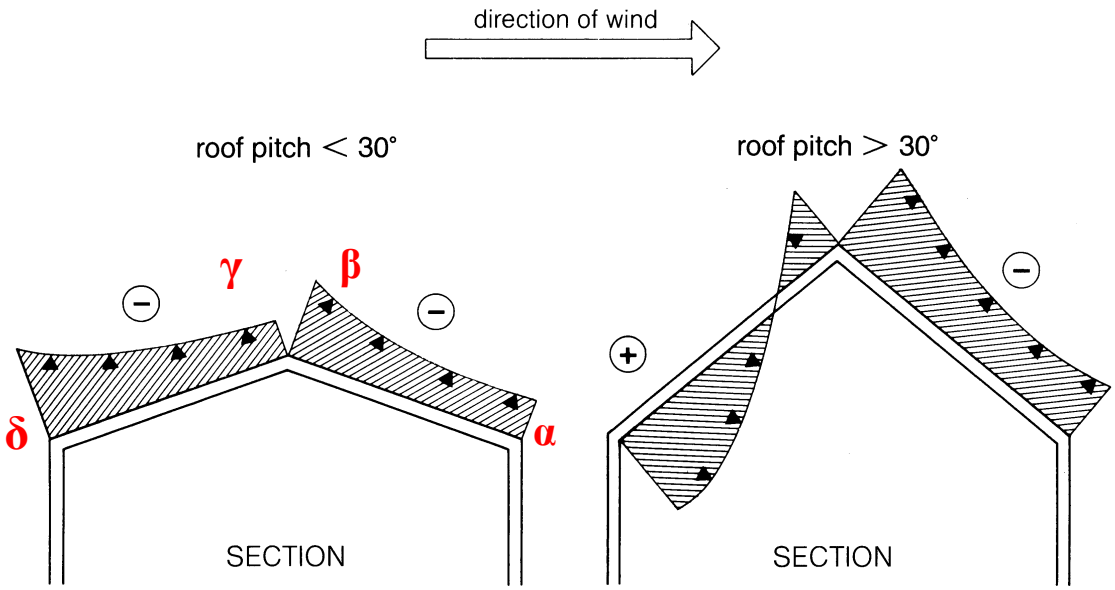

Figure 3.3 Wind pressure distribution according to roof pitch angle

Figure 48. Distribution of pressure generated by wind over the surface of a roof (Liddamet 1986). According to the pitch of the roof the generated pressure can be negative or positive.